Monthly Notices
of the
ROYAL ASTRONOMICAL SOCIETY

MNRAS **470,** 915–931 (2017)
Advance Access publication 2017 May 20

doi:10.1093/mnras/stx1241

Eclipsing binary stars with a δ Scuti component

F. Kahraman Aliçavuş,[1,2]★ E. Soydugan,[1,2] B. Smalley[3] and J. Kubát[4]

[1]*Faculty of Sciences and Arts, Physics Department,Canakkale Onsekiz Mart University, 17100 Canakkale, Turkey*
[2]*Astrophysics Research Centre and Ulupınar Observatory, Çanakkale Onsekiz Mart University, 17100 Çanakkale, Turkey*
[3]*Astrophysics Group, Keele University, Staffordshire ST5 5BG, UK*
[4]*Astronomický ústav, Akademie ved České republiky, CZ-251 65 Ondřejov, Czech Republic*

Accepted 2017 May 18. Received 2017 May 18; in original form 2016 November 8

ABSTRACT

Eclipsing binaries with a δ Sct component are powerful tools to derive the fundamental parameters and probe the internal structure of stars. In this study, spectral analysis of six primary δ Sct components in eclipsing binaries has been performed. Values of $T_{\rm eff}$, $v \sin i$, and metallicity for the stars have been derived from medium-resolution spectroscopy. Additionally, a revised list of δ Sct stars in eclipsing binaries is presented. In this list, we have only given the δ Sct stars in eclipsing binaries to show the effects of the secondary components and tidal-locking on the pulsations of primary δ Sct components. The stellar pulsation, atmospheric and fundamental parameters (e.g. mass, radius) of 92 δ Sct stars in eclipsing binaries have been gathered. Comparison of the properties of single and eclipsing binary member δ Sct stars has been made. We find that single δ Sct stars pulsate in longer periods and with higher amplitudes than the primary δ Sct components in eclipsing binaries. The $v \sin i$ of δ Sct components is found to be significantly lower than that of single δ Sct stars. Relationships between the pulsation periods, amplitudes and stellar parameters in our list have been examined. Significant correlations between the pulsation periods and the orbital periods, $T_{\rm eff}$, $\log g$, radius, mass ratio, $v \sin i$ and the filling factor have been found.

Key words: stars: atmospheres – binaries: eclipsing – stars: fundamental parameters – stars: oscillations – stars: variables: δ Scuti.

1 INTRODUCTION

The δ Scuti (δ Sct) stars are remarkable objects for asteroseismology particularly because of their pulsation mode variability. The δ Sct stars oscillate in low-order radial and non-radial pressure and gravity modes and most of them have frequency range of 5–50 d^{-1} (Breger 2000). Pulsations are driven by the κ-mechanism in these variables (Houdek et al. 1999). The δ Sct stars are dwarf to giant stars with spectral types between A0 and F0 (Chang et al. 2013). These variables have masses from 1.5 to 2.5 $M_{\odot}$ and are located on or near the main sequence (Aerts, Christensen-Dalsgaard & Kurtz 2010). Therefore, they are in a transition region where the convective envelope turns to a radiative envelope, while energy starts to be transferred by convection in the core of the star (Aerts et al. 2010). The δ Sct stars allow us to understand the processes occurring in this transition region by using their pulsation modes.

Approximately 70 per cent of stars are binary or multiple systems (Mason et al. 2009; Sana & Evans 2011; Alfonso-Garzón et al. 2014). Therefore, it is likely to find a δ Sct variable as a member of a binary system. The existence of a pulsating variable in an eclipsing binary system makes this variable more valuable. Using the pulsation characteristic, the interior structure of the star can be probed and, using the eclipsing characteristic, the fundamental parameters (e.g. mass, radius) of the pulsating component can be derived by modelling the light and radial velocity curves of a binary system. These fundamental parameters are important to make a reliable model of a pulsating star. Thus, the interior structures and the evolution statuses of stars can be examined in detail.

Many δ Sct stars in eclipsing binary systems have been discovered (e.g. Lee et al. 2016b; Soydugan et al. 2016). A group of eclipsing binaries with a δ Sct component was defined as oscillating eclipsing Algol (oEA) systems by Mkrtichian et al. (2004). The oEA systems are B to F type mass-accreting main-sequence pulsating stars in semidetached eclipsing binaries. Because of mass-transfer from the secondary components on to the primary pulsating stars and also due to the tidal distortions in oEA systems, the pulsation parameters and the evolution of primary pulsating components can be different.

There have been several studies on the effect of binarity on δ Sct type pulsations. First, Soydugan et al. (2006a) showed the effect of orbital period on the pulsation period. The relation between orbital and pulsation periods was theoretically revealed by Zhang, Luo & Fu (2013). They showed that pulsation periods vary depending on the orbital period, mass ratio of binary system, and filling factor of the primary pulsating component. It was also shown that the gravitational force applied by secondary components on to their

★ E-mail: filizkahraman01@gmail.com

primary components influences the pulsation periods of primary δ Sct components (Soydugan et al. 2006a). Because of the effects of mass-transfer and tidal distortions in semidetached binaries, the primary δ Sct components also evolve more slowly through the main sequence than single δ Sct stars (Liakos & Niarchos 2015).

The number of known binaries with a δ Sct component constantly increases. Additionally, hybrid stars, which show both δ Sct and γ Dor-type pulsations, have been discovered in eclipsing binary systems (Hambleton et al. 2013; Schmid et al. 2015). In a recent study, an updated list of δ Sct stars in binaries was presented by Liakos & Niarchos (2017). In their study, all known δ Sct stars and also δ Sct–γ Dor hybrids in binaries were collected, including the non-eclipsing ones. Although 199 binary systems are given in their list, there are only 87 detached and semidetached eclipsing binaries containing a δ Sct variable. The others are mostly visual binaries, ellipsoidal variables and spectroscopic binaries in which the fundamental parameters cannot be derived as precisely as in eclipsing binary systems.

As listed by Lampens (2006), some open questions about the eclipsing binaries with a pulsation component exist. The effect of binarity on pulsation quantities (period and amplitude) and possible connections between orbital motion, rotation, chemical composition and pulsation are some of these questions. Therefore, we have focused on the eclipsing binary systems with δ Sct components in this study. To obtain the stellar atmospheric parameters, a spectroscopic analysis of six δ Sct stars in eclipsing binary systems has been performed. A revised list of δ Sct stars in eclipsing binaries is presented to show the effects of secondary components and fundamental stellar parameters on the pulsations of the primary pulsating components.

Information about the spectroscopic observations and data reduction are given in Section 2. The spectroscopic analysis of the stars is presented in Section 3. The revised list of eclipsing binary systems with a δ Sct component, general properties of these systems and the relations between pulsation periods, amplitudes, and fundamental parameters of the stars are introduced in Section 4. In Section 5, we present a discussion on the correlations found, the positions of δ Sct stars in eclipsing binaries in the $\log T_{\rm eff}$–$\log g$ diagram and a comparison of the properties of single and eclipsing binary members δ Sct stars. The conclusions are given in Section 6.

2 OBSERVATIONS

Spectroscopic observations of six eclipsing binaries with a primary δ Sct component were carried out. The stars were selected taking into account the secondary components' light contributions, in order to obtain spectra that are less influenced by the light of secondary components. The light contributions of the stars from literature photometric analyses are given in Table 1.

The observations were carried out using the 2-metre Perek Telescope at the Ondřejov Observatory (Czech Republic). We acquired spectra with the coudé slit spectrograph at its 700-mm focus, in which the PyLoN 2048×512 BX CCD chip was used (for details, see Šlechta & Škoda 2002). The resolving power of the instrument is about 25 000 at 4300 Å. The spectra were taken in the wavelength range of 4272–4506 Å, which covers the H γ line. This wavelength region was also selected because metal lines (e.g. Ti , Mg, and Fe) are more numerous in this range of effective temperature.

To further minimize the light contribution of secondary components in the spectra, spectra of each star were taken at approximately 0.5 orbital phase when the primary is covering the secondary. The individual spectra were combined to increase the signal-to-noise (S/N) ratio. For CL Lyn, an ELODIE[1] spectrum, taken in 2001, was used in addition to our observation. Information about the spectroscopic survey is given in Table 1. The stars are semidetached eclipsing binaries with a primary δ Sct component, except for HZ Dra, which is a detached binary with a primary δ Sct component (Liakos et al. 2012).

Table 1. Information about the spectroscopic survey. S/N gives the values for combined spectra apart from CL Lyn. The S/N of CL Lyn is the value for ELODIE spectrum.

Name	Observation dates	S/N	Number of spectra	Light contribution[a]
XX Cep	2015-06/09	50	2	3.7 [1]
UW Cyg	2015-07/09	35	2	5.1 [2]
HL Dra	2015-06/07	120	2	4.4 [2]
HZ Dra	2015-06/07/09	80	3	0.5 [2]
TZ Dra	2015-06/09	60	2	7.6 [3]
CL Lyn	2015-09&2001	50	2	4.2 [2]

Notes. [a]Percentage of light contribution of secondary component in *B* band. [1] Koo et al. (2016), [2] Liakos et al. (2012), [3] Liakos & Niarchos (2013).

The reduction and normalization of the spectra were performed using the National Optical Astronomy Observatory (NOAO)/IRAF package.[2] In the reduction process, bias subtraction, flat-field correction, scattered light extraction, and wavelength calibration were applied. The reduced ELODIE spectrum for CL Lyn was used. The standard reduction was performed by the dedicated reduction pipeline of ELODIE. The spectra of each star were manually normalized using the *continuum* task of the NOAO/IRAF package.

3 SPECTROSCOPIC ANALYSIS

Prior to detailed spectroscopic analysis, spectral classifications of the stars were obtained. The effective temperature ($T_{\rm eff}$) of the primary components was derived using the spectral energy distribution (SED) and the H γ line. The metallicities were obtained using the spectrum fitting method.

3.1 Spectral classification

Preliminary information about the atmospheric parameters ($T_{\rm eff}$, surface gravity $\log g$) and surface peculiarities of stars can be obtained by spectral classification (Niemczura, Smalley & Pych 2014).

The spectral and luminosity types of stars are identified by comparing their spectra with a group of well-known standard stars' spectra. The A–F-type standard stars were used in our classification (Gray et al. 2003), because the δ Sct variables are A- and F-type stars. The spectral types of the stars were derived primarily using H γ and neutral metal lines (Fe, Ti) in the 4400–4500 Å wavelength region. The luminosity types were also derived by using the ionized metal lines.

The spectral and luminosity types obtained for the stars are given in Table 2. Only for HZ Dra, newly determined spectral classification (A8/A7 V) was found to be significantly different than the previous classification (A0, Heckmann 1975), while the other spectral types are mostly in agreement with the literature.

[1] http://atlas.obs-hp.fr/elodie/
[2] http://iraf.noao.edu/

Table 2. The stellar parameters of the six δ Sct stars in eclipsing binaries.

Name	V (mag)	$E(B-V)$ (mag) $\pm$ 0.023	Sp type (literature)	Sp type (This study)	$T_{\rm eff}$ (SED) (K)	$T_{\rm eff}$ (Spec) (K)	$\log g^a$	$v \sin i$ (km s^{-1})	$[m/H]$
HL Dra	7.36	0.040	A5[1]	A6 IV	7786 $\pm$ 174	7800 $\pm$ 200	4.22	107 $\pm$ 10	-0.12 ± 0.17
HZ Dra	8.14	0.016	A0[1]	A8/A7 V	7926 $\pm$ 250	7700 $\pm$ 200	4.07	120 $\pm$ 10	-0.09 ± 0.20
XX Cep	9.18	0.026	A6 V[2]	A7 V	7160 $\pm$ 152	8200 $\pm$ 300	4.09	54 $\pm$ 5	0.59 ± 0.23
TZ Dra	9.32	0.020	A7 V[3]	A7 V	7382 $\pm$ 173	7800 $\pm$ 200	4.26	86 $\pm$ 8	-0.01 ± 0.22
CL Lyn	9.77	0.181	A5[1]	A8 IV	7699 $\pm$ 189	7600 $\pm$ 300	3.98	75 $\pm$ 3	-0.16 ± 0.20
UW Cyg	10.86	0.101	A6V[4]	A7/A6 IV	7550 $\pm$ 176	7800 $\pm$ 350	4.06	45 $\pm$ 10	*

Notes. [a]Calculated using the stars' masses and radii that are given in Table A1. *Could not be calculated because of the low S/N ratio. [1] ESA (1997), [2] Koo et al. (2016), [3] Herbig (1960), [4] Liakos et al. (2012).

3.2 Determination of $T_{\rm eff}$, $v \sin i$ and metallicity

The $T_{\rm eff}$ of the primary δ Sct components were obtained from the H γ line and metallicities were determined using metal lines in the 4400–4500 Å wavelength region.

Prior to the spectral analysis, we determined $T_{\rm eff}$ from the SED. The SEDs were constructed from literature photometry and spectrophotometry, using 2MASS J, H, and K_s magnitudes (Sktrutskie et al. 2006), Tycho B and V magnitudes (Høg et al. 1997), USNO-B1 R magnitudes (Monet et al. 2003), TASS I magnitudes (Droege et al. 2006), and data from the Ultraviolet Sky Survey Telescope (TD1; Boksenberg et al. 1973). However, TD1 data are available for only HL Dra and HZ Dra. To remove the effect of interstellar reddening on the SED, $E(B-V)$ values were calculated from the Galactic extinction maps (Amôres & Lépine 2005), with distances obtained from *Gaia* parallaxes[3] (Casertano et al. 2017). The $E(B-V)$ values are given in Table 2. The average uncertainty in $E(B-V)$ was found to be 0.023 mag. The SEDs were dereddened using the analytical extinction fits of Seaton (1979) for the ultraviolet and Howarth (1983) for the optical and infrared.

The stellar $T_{\rm eff}$ (SED) values were determined by fitting solar-composition Kurucz (1993) model fluxes to the dereddening SEDs. The model fluxes were convolved with photometric filter response functions. A weighted Levenberg–Marquardt non-linear least-squares fitting procedure was used to find the solution that minimized the difference between the observed and model fluxes. Since $\log g$ is poorly constrained by our SEDs, we fixed $\log g = 4.0$ for all the fits. The uncertainties in $T_{\rm eff}$ (SED) include the formal least-squares error and uncertainties in $E(B-V)$ (0.023) and $\log g$ (0.2) added in quadrature. In Fig. 1 , we show the SED fit for HL Dra.

By using the initial values of $T_{\rm eff}$ (SED), fundamental atmospheric parameters were determined for each star. Before the hydrogen line analysis and metallicity determinations of the stars, the projected rotational velocity ($v \sin i$) values were derived. A theoretical spectrum of each star was calculated using the initial atmospheric parameters. The metal lines in the spectrum of each star were matched to the theoretical spectrum by adjusting $v \sin i$ (Gray 2008). Final values of $v \sin i$ were obtained by minimizing the difference between the observed and theoretical spectra. The $v \sin i$ values are given in Table 2.

Hydrogen lines are good temperature indicators, since they are insensitive to $\log g$ for stars with $T_{\rm eff} < 8000$ K (Heiter et al. 2002; Gray 2008). In our analysis, we adopted value of $\log g$ that were calculated using the stars' masses and radii values given in the literature (see Table A1). Additionally, $v \sin i$ and metallicity ($[m/H]$, assumed to be solar) were fixed. In our analysis, the hydrostatic, plane-parallel, local thermodynamic equilibrium ATLAS9 models (Kurucz 1993) were used and the SYNTHE code (Kurucz & Avrett 1981) was used to produce theoretical spectra. $T_{\rm eff}$ was determined by minimizing the difference between the theoretical and observed hydrogen line, as described by Catanzaro, Leone & Dall (2004). The $T_{\rm eff}$ (Spec) values obtained are listed in Table 2 and comparison of the calculated and observed spectra for one of the stars is shown in Fig. 2.

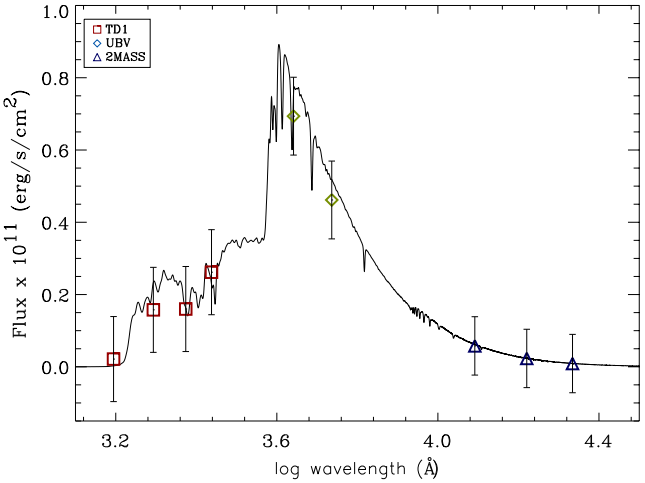

Figure 1. SED fit for HL Dra.

The $[m/H]$ values were derived using the $T_{\rm eff}$ (Spec), $\log g$, and $v \sin i$ values given in Table 2. The analysis was executed using version 412 of the Spectroscopy Made Easy (SME) package (Valenti & Piskunov 1996), which determines atmospheric parameters, $[m/H]$ and elemental abundances using the spectrum fitting method. In this analysis, atmosphere models produced by ATLAS9 code (Kurucz 1993) were used. The line list was taken from the Vienna Atomic Line Data base[4] (VALD; Piskunov et al. 1995). The 4400–4500 Å wavelength range was used in the metallicity analysis. The $[m/H]$ values obtained are given in Table 2. However, $[m/H]$ could not be determined for UW Cyg because of the low S/N ratio of the spectra. The comparison of the theoretical and observed spectra used in the $[m/H]$ analysis is demonstrated in Fig. 3. Uncertainties of the spectroscopic parameters comprise the least-squares error and the uncertainties caused by the fixed parameters in each analysis.

[3] https://gea.esac.esa.int/archive/

[4] http://vald.astro.uu.se/

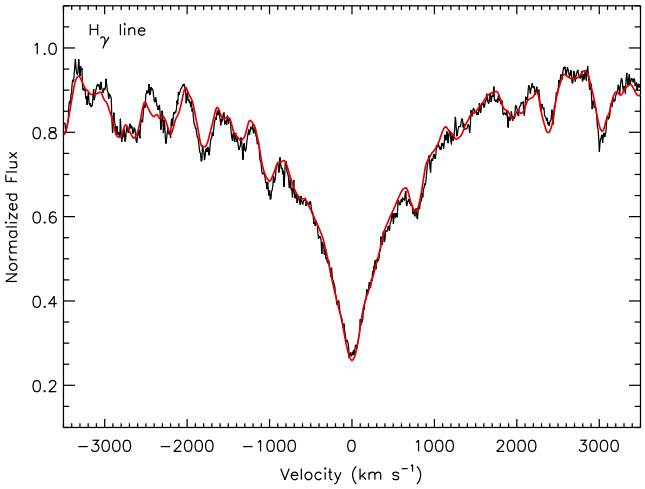

Figure 2. Comparison of the calculated (red line) and observed spectra of H γ line of HL Dra.

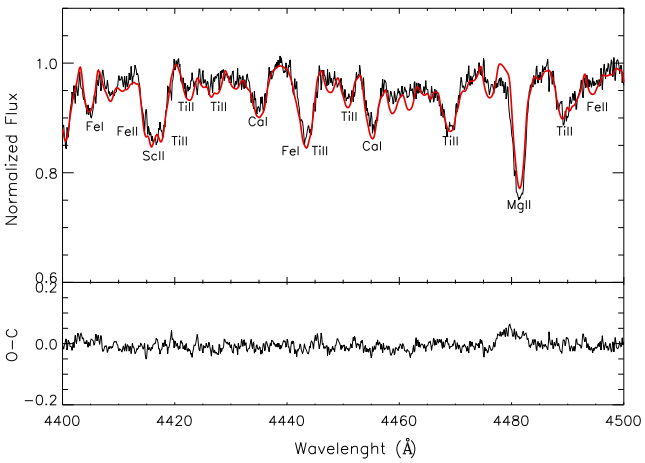

Figure 3. Upper panel: comparison of the theoretical (red lines) and observed spectra of HL Dra. Lower panel: difference between the observed and theoretical spectra.

Additionally, the error due to low S/N ratio was included, using the value from Kahraman Aliçavuş et al. (2016).

The $T_{\rm eff}$ values of the analysed stars were also compared with those used in the literature. In this comparison, we noticed that if $T_{\rm eff}$ had been obtained from spectral classifications, the $T_{\rm eff}$ used in previous studies are in agreement with our spectroscopic results to within the errors. Others, however, have completely different values. We determined $T_{\rm eff}$ values of HZ Dra and XX Cep to be 7700 and 8200 K, respectively. However, their previously used $T_{\rm eff}$ values are 9800 K for HZ Dra (Liakos et al. 2012) and 7300 K for XX Cep (Hosseinzadeh, Pazhouhesh & Yakut 2014). However, a newer spectral analysis of XX Cep was recently presented by Koo et al. (2016). They obtained $T_{\rm eff} = 7946 \pm 240$ K and $v \sin i = 48.6 \pm 6.8$ km s^{-1}, which are in good agreement with our results.

4 δ SCT STARS IN ECLIPSING BINARY SYSTEMS

The properties of δ Sct stars in eclipsing binaries can be different from single δ Sct stars. Especially, the pulsating primary components in close binary systems evolve differently than single ones (Liakos & Niarchos 2015). In close binary systems, the primary component can gain mass from the secondary and can be covered by material from the secondary. Additionally, tidal distortion is present in these systems. Mass-transfer and tidal distortion will affect the pulsation period ($P_{\rm puls}$) and amplitude (*Amp*) of δ Sct stars in close binaries. How much the binarity affects the δ Sct pulsations in binaries is one of the open questions.

To show the effect of binarity on pulsation, the correlations between $P_{\rm puls}$, *Amp* and the orbital and atmospheric parameters of eclipsing binary member δ Sct stars have been examined. First, a correlation between $P_{\rm puls}$ and orbital period ($P_{\rm orb}$) for 20 δ Sct stars in eclipsing binaries was found by Soydugan et al. (2006a). The $P_{\rm puls}$–$P_{\rm orb}$ correlation was improved by newer discoveries (Liakos et al. 2012). Then, a theoretical explanation for the $P_{\rm puls}$–$P_{\rm orb}$ correlation was given by Zhang et al. (2013), who expressed $P_{\rm puls}$ mainly as a function of the pulsation constant (Q), the filling factor (f), $P_{\rm orb}$, and the mass ratio ($q = M_{\rm secondary}/M_{\rm primary}$, where M denotes the mass) with the following equation:

$$P_{\rm puls} = \frac{G^{1/2}}{2\pi} Q f^{3/2} r^{3/2} (1+q)^{1/2} P_{\rm orb}, \quad (1)$$

where G and r are the gravitational constant and effective radius (radius divided by semimajor axis), respectively. f shows how much a star fills its Roche potential (Ω) and it is expressed by

$$f = (\Omega_{\rm inner} - \Omega)/(\Omega_{\rm outer} - \Omega_{\rm inner}). \quad (2)$$

Zhang et al. (2013) tested whether this theoretical approach is compatible with the observed correlation of $P_{\rm puls}$–$P_{\rm orb}$ using 69 eclipsing binaries with δ Sct stars. They found that the theoretical correlation is in agreement with the observed one. This correlation was also confirmed by Liakos & Niarchos (2017). They obtained a similar correlation using 66 semidetached and 25 detached systems that have $P_{\rm orb} \leq 13$ d. They also showed that for binaries with $P_{\rm orb} > 13$ d, there is no significant effect of binarity on pulsations. In their study, the known correlation between $P_{\rm puls}$ and $\log g$ was also shown for 82 systems that contained semidetached, detached, and unclassified stars with $P_{\rm orb} < 13$ d. However, it should be kept in mind that in their study, both eclipsing and non-eclipsing binaries were used and some of these stars were assumed to be detached systems. Additionally, a negative correlation between $P_{\rm puls}$ of primary δ Sct components and gravitational force applied by secondary components on to the pulsating stars has been found (Soydugan et al. 2006a; Liakos et al. 2012; Liakos & Niarchos 2017).

The known and possible correlations between the fundamental absolute parameters (e.g. masses, radii), atmospheric parameters and the pulsation quantities ($P_{\rm puls}$, *Amp*) of δ Sct components in eclipsing binary systems give us an opportunity to understand these stars in detail and show the effect of secondary components, mass-transfer, and tidal-locking on pulsation quantities. Therefore, we have prepared a revised list of eclipsing binaries with a primary δ Sct component. The list includes 67 semidetached and 25 detached eclipsing binaries. Seven of these stars (WX Dra, GQ Dra, KIC 06669809, KIC 10619109, KIC 1175495, KIC 10686876, and KIC 6629588) were taken from Liakos & Niarchos (2016, 2017). In these studies, the stars were found to be δ Sct variables in eclipsing binaries for the first time. In our study, we did not include any stars that have unclassified Roche geometry.

The parameters of the primary and secondary components of our sample of 92 eclipsing binary systems with a primary δ Sct component were gathered from the literature. In this revised list, values of $T_{\rm eff}$, $\log g$, masses (M), radii (R), luminosities (L), bolometric

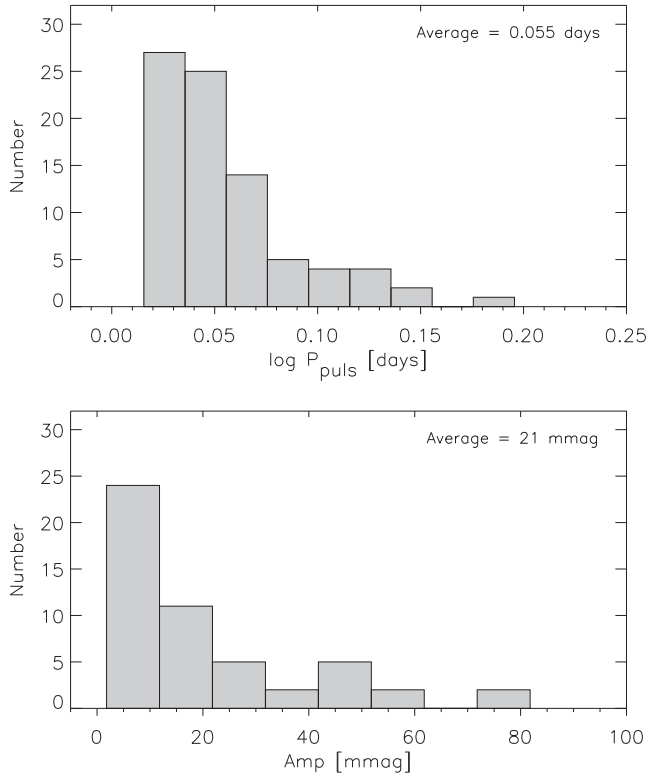

Figure 4. The distributions of P_{puls} and V-band *Amp* of the primary δ Sct components in eclipsing binary systems.

magnitudes (M_{bol}), semimajor axis (a) of the primary and secondary components and f, $v \sin i$, P_{puls}, peak-to-peak *Amp* in V and B band of primary pulsating components and the parallaxes, orbital inclinations (i) and the q of binary systems were collected, as well as the basic parameters of the systems such as visual magnitudes (V), spectral types (SP), and binary types. This updated list contains more stars and a wider variety of stellar parameters than the previous list (Liakos & Niarchos 2017). The updated list is given in Table A1.

4.1 General properties of δ Sct components in eclipsing binaries

In our list, there are only two eclipsing binaries that show δ Sct type pulsations in both components (RS Cha and KIC 09851944). In the other eclipsing binaries, only the primary components exhibit δ Sct type pulsations. Therefore, in all our examinations, we took into account only the properties of the primary δ Sct components.

The P_{puls} and V-band *Amp* distributions of primary δ Sct components in eclipsing binaries are shown in Fig. 4. The pulsation periods of the highest amplitudes were collected in the list and only V-band *Amp* of the stars was used in any comparisons and analyses in this study. It is clearly seen that δ Sct-type primary pulsating components mainly oscillate in periods between ∼0.016 and 0.195 d, with an average amplitude of 21 mmag. In the list, there is also a high-amplitude δ Sct star (HADS, V1264 Cen) that is not used in Fig. 4 and excluded in the next steps. The average P_{puls} values for semidetached and detached systems were found to be 0.049 and 0.073 d, respectively. Although the number of detached systems is lower than the semidetached ones, there is a clear distinction between the pulsation periods of both systems. However, we did not find a significant difference in the V-band *Amp* of δ Sct components of both type of eclipsing binary. The reason for lower pulsation periods of primary δ Sct components in the semidetached systems can be the effects of tidal-locking and mass-transfer from the secondary non-pulsating component to the primary pulsating component (Soydugan et al. 2003, 2006b; Liakos et al. 2012). The primary component gains mass from the secondary component and this can change the surface composition and internal structure of the primary pulsating component and also the angular momentum of both components changes during this process (Aerts et al. 2010). Hence, mass-transfer could affect the oscillations.

The T_{eff}, $\log g$ and $v \sin i$ ranges of δ Sct components in eclipsing binary systems are illustrated in Fig. 5. In the figure, the distributions of parameters obtained from photometric and spectroscopic studies are shown. Both photometric and spectroscopic T_{eff} and $\log g$ values have similar ranges, which are 6750–9660 K and 3.40–4.38, respectively. The $\log g$ values of semidetached and detached systems are in the range of 3.80–4.38 and 3.50–4.20, respectively,

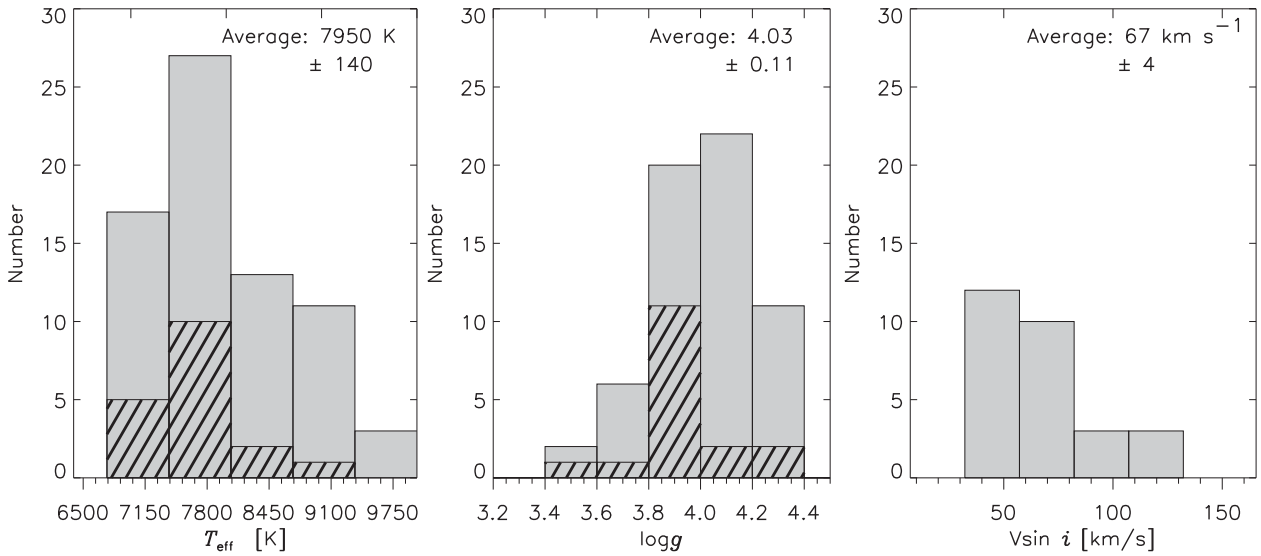

Figure 5. The distributions of T_{eff}, $\log g$ and $v \sin i$ values of primary δ Sct components in eclipsing binaries. The grey histograms show the distributions of whole sample, while slanted lines represent the distributions of the stars that have T_{eff} and $\log g$ values derived by the spectroscopic analyses.

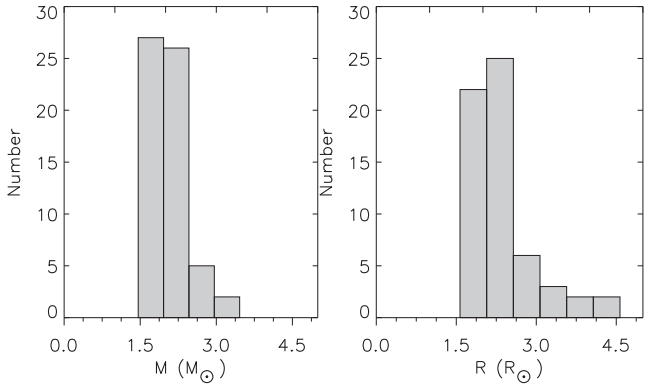

Figure 6. The distributions of M and R values of primary δ Sct components in eclipsing binaries.

while $T_{\rm eff}$ ranges of these eclipsing binary types are similar. One semidetached system, QY Aql, has a $\log g$ value of 3.40 (Liakos & Niarchos 2013), which is low for the primary component of a semidetached system, since they are generally main-sequence stars. The $v \sin i$ values of the primary δ Sct components were found to be in the range from 12 to 130 km s^{-1}. The values of M and R for the primary δ Sct components were also found in the ranges of 1.46–3.30 M$_\odot$ and 1.57–4.24 R$_\odot$, respectively, as shown in Fig. 6. No significant difference was obtained between the range of M and R values for detached and semidetached systems.

4.2 Correlations between the collected parameters and the pulsation quantities

The known and possible correlations between the collected fundamental, atmospheric and orbital parameters and the pulsation quantities of the primary δ Sct components in eclipsing binary systems were examined. First, the known correlation between $P_{\rm puls}$ and $P_{\rm orb}$ was checked for semidetached and detached systems. These correlations are demonstrated in Fig. 7. Average errors in $P_{\rm puls}$ and $P_{\rm orb}$ are about 10^{-3} and 10^{-5} d, and the error bars are smaller than the size of the symbols. Therefore, the error bars of $P_{\rm puls}$ and $P_{\rm orb}$ are not shown in this and subsequent figures. Additionally, for some stars, the errors of the parameters were not given in the literature. Therefore, the average uncertainties of the parameters are shown in all figures.

Significant positive $\log P_{\rm puls}$–$\log P_{\rm orb}$ correlations were found for both semidetached and detached systems. The relationships for these correlations are given in the top of each panel in Fig. 7. The correlation for semidetached systems was found to be stronger than for the detached systems. As can be seen from Fig. 7, all stars are mainly inside the 1σ level. The V-band pulsation Amp relation with $P_{\rm orb}$ was examined as well. As a result, a correlation was found between these parameters as shown in Fig. 8. However, the correlation is not strong because of the scatter and number of data points.

The correlations between the atmospheric parameters ($T_{\rm eff}$, $\log g$) and $P_{\rm puls}$ and V-band Amp of primary δ Sct components were examined. While no correlation between Amp and the atmospheric parameters was found, there are significant correlations between $T_{\rm eff}$, $\log g$ and $P_{\rm puls}$. As shown in Fig. 9, these correlations were found for all types of eclipsing binaries' primary δ Sct components and they show a negative variation in $P_{\rm puls}$ with increasing $T_{\rm eff}$ and $\log g$. However, as can be seen from the upper panel of Fig. 9, the $\log T_{\rm eff}$–$\log P_{\rm puls}$ relation is stronger for the pulsating primary components of detached systems than for semidetached systems.

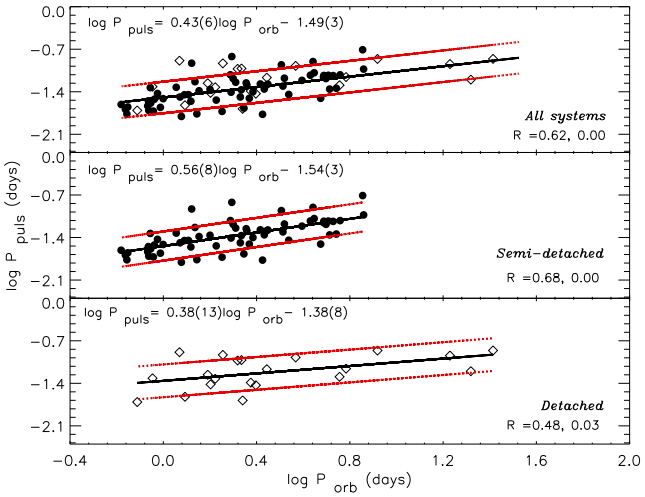

Figure 7. The correlations between $P_{\rm puls}$ and $P_{\rm orb}$ for detached (lower panel), semidetached (middle panel), and all systems (upper panel). The filled circles, diamonds, and red lines represent the semidetached, detached, and 1σ levels, respectively. The equations in each panel were obtained from the correlations. R constant shows the Spearman rank, which gives the strength of correlation (number before the comma in the R constant) and the deviation amount of points from the correlation (number after the comma in the R constant).

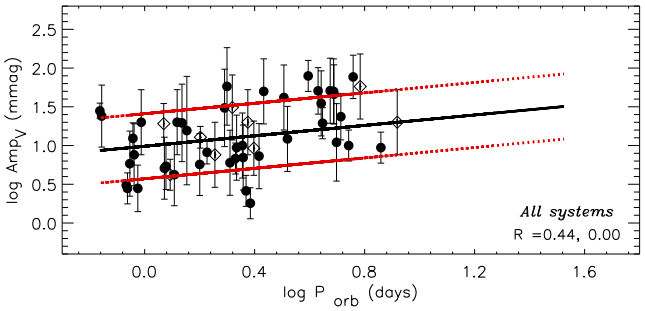

Figure 8. The correlation between the V-band pulsation Amp and $P_{\rm orb}$ of primary δ Sct stars in eclipsing binary systems. The symbols, lines, and the R constant are the same as in Fig. 7.

Therefore, only the relationship for the correlation for detached systems is given in Fig. 9. The $\log g$–$\log P_{\rm puls}$ relationship and the correlation for the primary δ Sct components in all types of eclipsing binary systems are also shown in Fig. 9.

The existence of $\log g$–$\log P_{\rm puls}$ correlation offers us other probable connections between M, R and $P_{\rm puls}$. Given that $\log g \propto M/R^2$, a positive correlation for R–$\log P_{\rm puls}$ and a negative correlation for M–$\log P_{\rm puls}$ should exist. Hence, these were examined and the expected correlations were obtained as demonstrated in Fig. 10. The positive R–$\log P_{\rm puls}$ correlation is stronger than the negative M–$\log P_{\rm puls}$ correlation. Additionally, no meaningful M and R correlations with V-band Amp were detected for all types of binaries with primary δ Sct components.

According to equation (1), theoretically a correlation between $P_{\rm puls}$ and q should exist. When this relation was examined, it turned out that a correlation is present for detached systems, although no significant correlation is found for semidetached systems. These are shown in the upper panel of Fig. 11. The $v \sin i$–$\log P_{\rm puls}$ correlation was examined as well. This correlation is also not significant for semidetached systems, while there is a strong correlation between

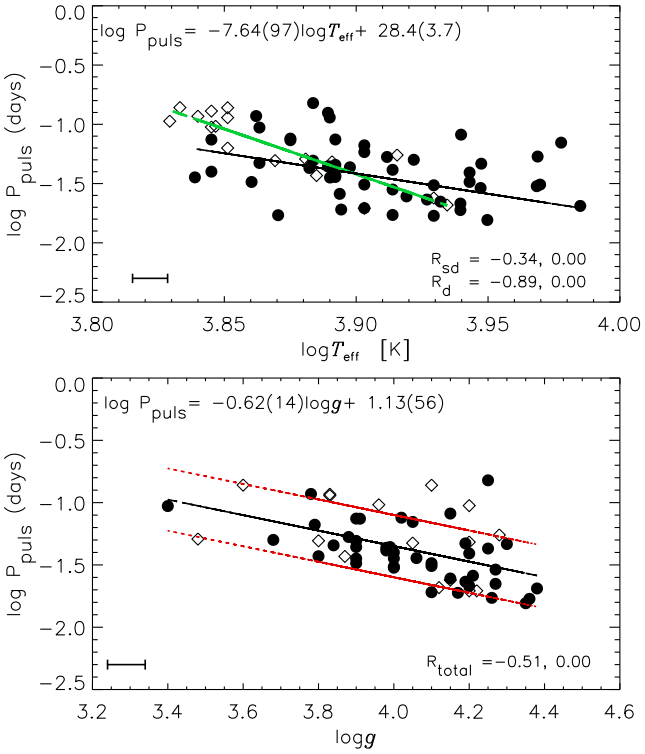

Figure 9. The $\log T_{\rm eff}$–$\log P_{\rm puls}$ (upper panel) and $\log g$–$\log P_{\rm puls}$ (lower panel) correlations. Green line in upper panel illustrates the correlation only for detached systems, while black line shows the correlation of semidetached systems. The equations in upper and lower panels are given for detached and all systems' primary δ Sct components considering the correlations, respectively. The symbols, red lines and R constant are the same as in Fig. 7.

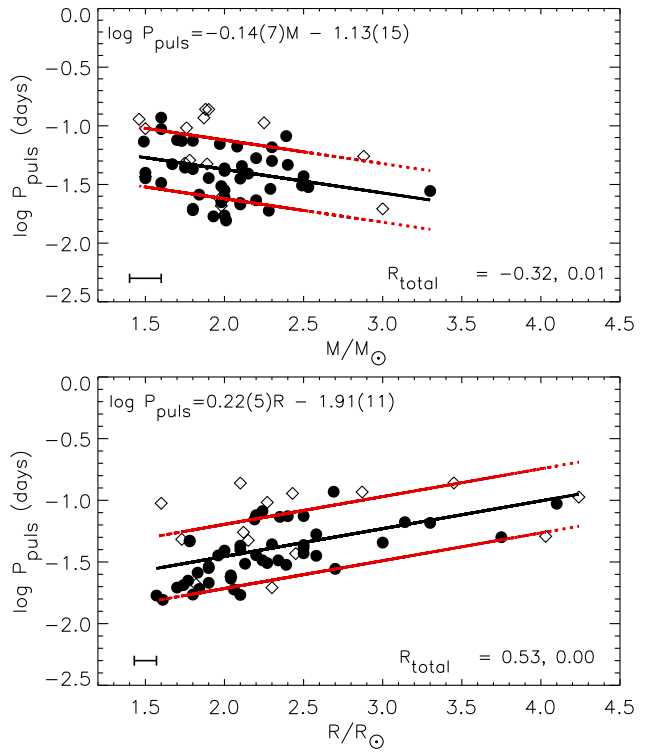

Figure 10. The M–$\log P_{\rm puls}$ (upper panel) and R–$\log P_{\rm puls}$ (lower panel) correlations. The equation in lower panel was derived from the correlation for both detached and semidetached systems. The symbols, red lines and R constant are the same as in Fig. 7.

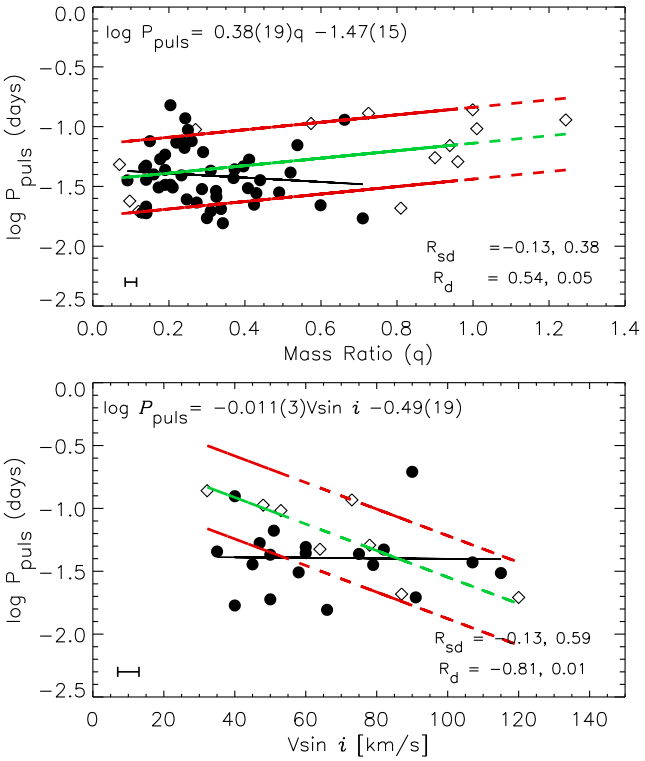

Figure 11. The q–$\log P_{\rm puls}$ (upper panel) and $v \sin i$–$\log P_{\rm puls}$ (lower panel) correlations. Green lines illustrate the correlations for detached systems, while black lines show semidetached systems' correlations. The equations in each panel were derived from the correlations of detached systems. The symbols, red lines, and R constant are the same as in Fig. 7.

$v \sin i$ and $P_{\rm puls}$ for detached systems. This relation is shown in the lower panel of Fig. 11.

The other important factor that theoretically affects $P_{\rm puls}$ according to equation (1) is the filling factor (f) of primary δ Sct components. A direct proportional relation between f and $P_{\rm puls}$ should exist. When this relation was examined for semidetached systems, f was found to be inversely related to $P_{\rm puls}$ as shown in the upper panel of Fig. 12. This result conflicts with equation (1). We also investigated the f–$P_{\rm orb}$ correlation. As shown in the lower panel of Fig. 12, f regularly decreases with increasing $P_{\rm orb}$.

Additionally, we calculated the gravitational force (F) that is applied by the secondary component to the primary pulsating δ Sct star. The effect of this force causes a decrease in $P_{\rm puls}$. This result was first obtained by Soydugan et al. (2006a). They found the same result as we show in the right-hand, upper panel of Fig. 13. The relation between F- and V-band pulsation Amp was examined as well and a negative correlation was found. The relationships for these correlations were found to be

$$\log P_{\rm puls} = -0.25(6)F - 0.75(17) \quad (3)$$

$$\log Amp = -0.29(15)F + 1.76(42). \quad (4)$$

In the left-hand panel of Fig. 13, we show the correlations between orbital separation (a), $P_{\rm puls}$ and V-band Amp values. These correlations are opposite to the correlations found for F as expected, because $F \propto a^{-2}$.

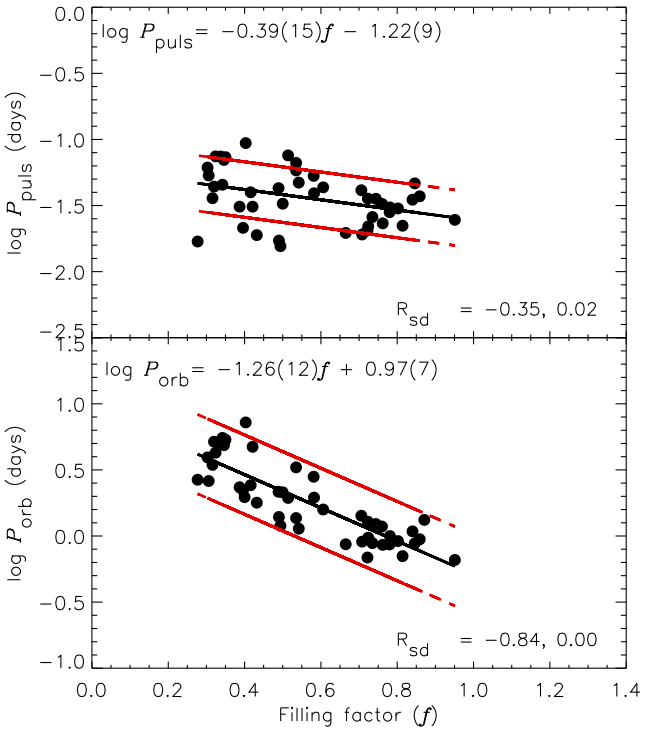

Figure 12. The correlation between P_{puls}, P_{orb} and f. The equations in the panels were derived from the correlations for semidetached systems. No errors of f values were given in the literature, hence we could not show the error bars of f values. The symbols, red lines and R constant are the same as in Fig. 7

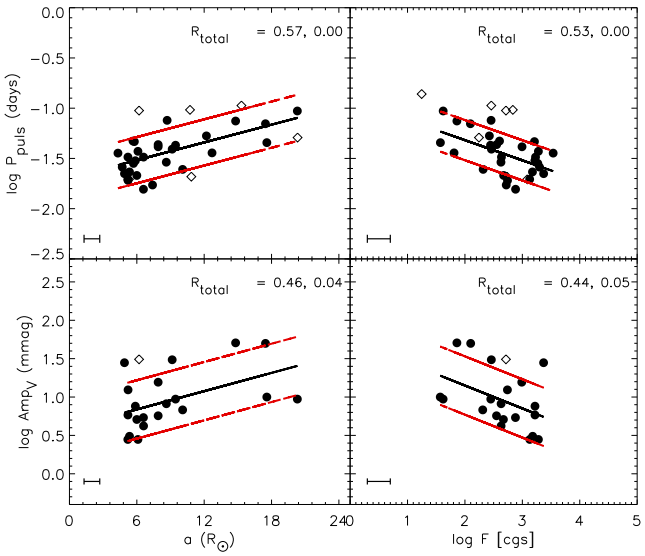

Figure 13. The correlations of a and F with the P_{puls} and V-band pulsation Amp values. The symbols, red lines and R constant are the same as in Fig. 7.

5 DISCUSSION

5.1 Comparison of single and eclipsing binary member δ Sct stars

In this section, we compare the properties of single and eclipsing binary member δ Sct stars. All parameters of single δ Sct stars were taken from Rodríguez, López-González & López de Coca (2000, R2000, hereafter).

The P_{puls} values of δ Sct components in eclipsing binaries were found between ∼0.016 and 0.147 d, while the P_{puls} range for single δ Sct stars extends to 0.288 d (R2000). Hence, P_{puls} values of single δ Sct stars are significantly longer than those in eclipsing binaries. Additionally, highest V-band Amp value of single δ Sct stars is 250 mmag (R2000), compared to only 80 mmag for δ Sct stars in eclipsing binaries.[5] This difference was mentioned in the study of Soydugan et al. (2006b). Furthermore, the binarity effect was found when the average values of P_{puls} of semidetached and detached systems were compared. Oscillations of δ Sct stars in detached systems were found to be slower (∼0.073 d^{-1}) than for semidetached systems (∼0.045 d^{-1}). Because semidetached systems have generally lower P_{orb} values than detached systems, tidal-locking is more effective in these systems. Additionally, in semidetached systems the secondary components are evolved stars and they transfer mass on to the primary pulsation components. However, no difference was found between the V-band pulsation Amp of detached and semidetached systems. The reason of this could also be the effect of mass-transfer in semidetached systems.

The T_{eff} and log g of δ Sct components in eclipsing binaries were found in the ranges of 6750–9660 K and 3.40–4.38, respectively. All types of eclipsing binary member δ Sct stars have the same T_{eff} ranges, although the evolved stars, which have log g values lower than 3.80, are generally detached-type eclipsing binary systems, except for QY Aql that probably has an incorrect log g value. The T_{eff} of δ Sct stars is typically in the range of 6300–8600 K (Uytterhoeven et al. 2011). The values of δ Sct stars in eclipsing binaries are in a good agreement with this range. However, there are some hotter stars and the T_{eff} of these stars should be re-examined. Comparisons of T_{eff} and log g for single and eclipsing binary member δ Sct stars were not made, owing to a lack of these parameters for single δ Sct stars in R2000.

The v sin i values of primary δ Sct components in eclipsing binary systems were found between 12 and 130 km s^{-1} but extend to 285 km s^{-1} for single δ Sct stars (R2000). The average v sin i values for single and binary member δ Sct stars are 90 and 64 km s^{-1}, respectively. As a whole, the single δ Sct stars rotate faster than those in eclipsing binary systems.

5.2 Correlations

A positive correlation between P_{puls} and P_{orb} was found for both detached and semidetached eclipsing binaries' primary δ Sct components. According to this correlation, P_{puls} of primary δ Sct components increase with the growing P_{orb}. Growing P_{orb} values relate to increasing a ($P_{orb} \propto a^{3/2}$). Therefore, the effect of the secondary component on the primary pulsating component decreases with increasing P_{orb} and the pulsations of the primary δ Sct stars are less influenced by binarity.

The P_{puls}–P_{orb} correlation was shown in the recent study of Liakos & Niarchos (2017) for all known δ Sct stars in binaries, including the non-eclipsing ones. They found that there is a 13-d limit in P_{orb} and for longer P_{orb} values, binarity has less of an effect on pulsations. However, our result is different. In our P_{puls}–P_{orb} correlation, there are detached stars (GK Dra, KIC 3858884, and KIC 8569819) that have $P_{orb} > 13$ d and agree with the P_{puls}–P_{orb} correlation to within the 1σ level. The 13-d P_{orb} limit for the binarity effect on pulsations appears to be underestimated. Our results show that binarity still influences the pulsations of primary δ Sct components with

[5] HADS stars were omitted in the comparison.

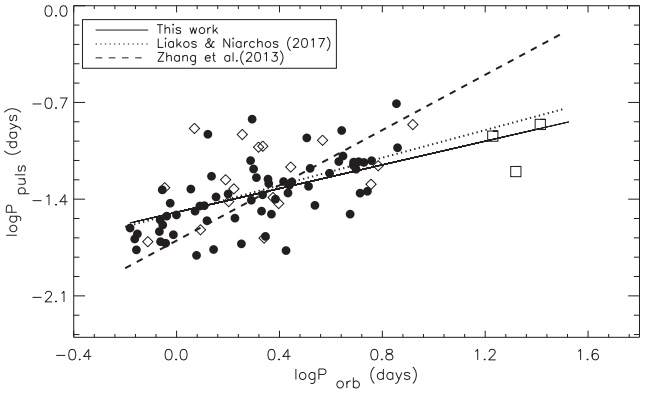

Figure 14. Comparison of $\log P_{\rm orb}$–$\log P_{\rm puls}$ correlations for eclipsing binaries with a primary δ Sct component. Square symbols illustrate that the stars have $P_{\rm orb} > 13$ d. The other symbols are the same as in Fig. 7.

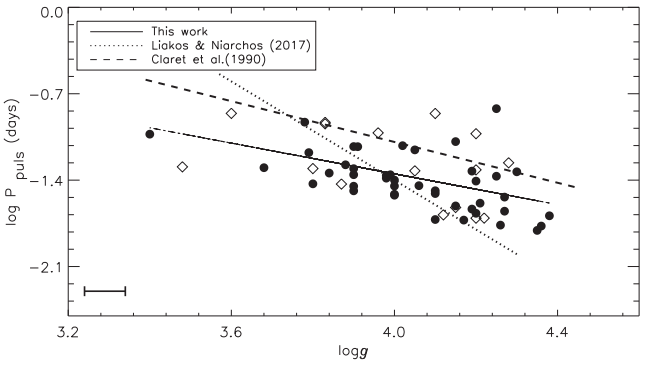

Figure 15. Comparison of $\log g$–$\log P_{\rm puls}$ correlations of single and eclipsing binary member δ Sct stars. The symbols are the same as in Fig. 7.

$P_{\rm orb} > 13$ d. Although Liakos & Niarchos (2017) did not include stars having $P_{\rm orb} > 13$ d in their $\log P_{\rm orb}$–$\log P_{\rm puls}$ correlation, our correlation is in agreement, as can be seen from Fig. 14. However, the theoretically calculated $\log P_{\rm orb}$–$\log P_{\rm puls}$ relationship by Zhang et al. (2013) is different than ours. The reason of this difference could be the negative effects of some parameters (f and q in semidetached systems) on the pulsations, contrary to the expected positive effects of these parameters according to equation (1), which were used to derive the theoretical $P_{\rm puls}$–$P_{\rm orb}$ relationship.

The V-band *Amp* of primary δ Sct components in eclipsing binary systems increases with increasing $P_{\rm orb}$. No *Amp*–$P_{\rm orb}$ correlation was found in previous studies (Soydugan et al. 2006a; Liakos et al. 2012; Zhang et al. 2013; Liakos & Niarchos 2017). The gravitational force applied by secondary components on to the surface of primary pulsation stars appears to cause a decrease in *Amp*.

A significant negative correlation was found between $T_{\rm eff}$ and $P_{\rm puls}$. Balona & Dziembowski (2011) also showed the same relation and Kahraman Aliçavuş et al. (in preparation) also found it for single δ Sct stars. The $T_{\rm eff}$ and $P_{\rm puls}$ relation is an expected result. When the pulsation constant ($Q = P_{\rm puls}(\overline{\rho}/\overline{\rho}_{\odot})^{0.5}$), mean density ($\overline{\rho} \sim M/R^3$), and the luminosity–mass relation ($L/{\rm L}_{\odot} \approx M/{\rm M}_{\odot}$) are taken into account, a negative relation between $P_{\rm puls}$ and $T_{\rm eff}$ is found ($P_{\rm puls} \propto (R/{\rm R}_{\odot})^{0.5}(T_{\rm eff}/T_{\rm eff\,\odot})^{-2}$). Additionally, changes in $T_{\rm eff}$ bears on the changes in R, which affect the region of He ionization that is responsible from the pulsations (Cox 1980).

The known negative correlation between $\log g$ and $P_{\rm puls}$ was demonstrated using the data of newly discovered stars. The correlation shows that main-sequence δ Sct components in eclipsing binaries pulsate in shorter periods than evolved stars. Using the pulsation constant, mean density, and surface gravity ($g \sim M/R^2$), a relationship between $P_{\rm puls}$ and g can be found ($P_{\rm puls} \propto g^{-0.5}\,R^{0.5}$). According to this rough approach, our $\log g$–$\log P_{\rm puls}$ correlation was found as expected.

The $\log g$–$\log P_{\rm puls}$ correlation was also examined by Liakos & Niarchos (2017) for δ Sct components in binary systems. Additionally, Claret et al. (1990) obtained the same relation for single δ Sct stars. In Fig. 15, we compare the correlations of $\log g$–$\log P_{\rm puls}$ found for single and binary δ Sct stars. Our correlation is approximately parallel to the correlation found for single δ Sct stars, but there is a significant difference between our correlation and that of Liakos & Niarchos (2017). In our study, we used only δ Sct stars in eclipsing binaries, whereas Liakos & Niarchos (2017) used all binaries containing δ Sct components. In eclipsing binaries, the $\log g$ values of pulsating components can be derived more accurately, which is probably the reason for the difference between the two correlations.

Positive R–$\log P_{\rm puls}$ and negative M–$\log P_{\rm puls}$ correlations were obtained, as expected. From the $\log g$–$\log P_{\rm puls}$ correlation, we know that both M and R values have effect on pulsation. Therefore, combining both equations we obtain

$$\log P_{\rm puls} = 0.11(R/{\rm R}_{\odot}) - 0.07(M/{\rm M}_{\odot}) - 1.52. \quad (5)$$

A similar equation was found for Cepheid stars by Fernie (1965). As can be seen from the equation, $P_{\rm puls}$ is more influenced by changes in R than changes in M. In Fig. 10, the weak effect of M and the stronger effect of R on the pulsation of primary δ Sct components can be seen.

We found that the binary mass ratio (q) has no significant effect on $P_{\rm puls}$ of primary δ Sct components in semidetached systems, although there is a correlation between q and $P_{\rm puls}$ for primary δ Sct components in detached systems. According to equation (1), $P_{\rm puls}$ should be directly proportional to q. The lack of any correlation in semidetached systems might be due to the lack of systems with $q > 0.5$.

The variation of $P_{\rm puls}$ with $v \sin i$ was also found only for detached systems. The $P_{\rm puls}$ decreases with increasing $v \sin i$. Since semidetached systems are generally close binaries, rotation synchronization is present. Therefore, owing to the $P_{\rm puls}$–$P_{\rm orb}$ correlation, we expected to find a correlation between $P_{\rm puls}$ and $v \sin i$ in the semidetached systems. However, mass-transfer in these systems is very effective and this changes the q and R of the primary δ Sct components, and these affect the rotation and angular momentum. The altered angular momentum also results in a change of $P_{\rm orb}$ that can change the rotation ($P_{\rm orb} = \sqrt{2\pi}/\omega$). All these effects can be the reason why we did not find a $v \sin i$–$P_{\rm puls}$ correlation for semidetached systems. A correlation between $P_{\rm puls}$ and $v \sin i$ was also found by Tkachenko et al. (2013) using the $v \sin i$ values of some δ Sct stars taken from Uytterhoeven et al. (2011) and R2000. In their work, they found a weak $P_{\rm puls}$–$v \sin i$ relation but, contrary to our results, with $P_{\rm puls}$ increasing with declining $v \sin i$. The rotation of stars causes changes in their stellar structure, hence the reason why $P_{\rm puls}$ can be different for different values of $v \sin i$ (Soufi, Goupil & Dziembowski 1998).

According to equation (1), f should be directly proportional to $P_{\rm puls}$. However, in our study, we have obtained the opposite result. When the correlation between $P_{\rm orb}$ and f was examined, we noticed that f increases with decreasing $P_{\rm orb}$. The gravitational force applied on the primary pulsating component grows with increasing f value. Thus, we can say, $P_{\rm orb}$ has a significant effect on f and we, therefore, obtained a negative relation between $P_{\rm puls}$ and f instead of a positive

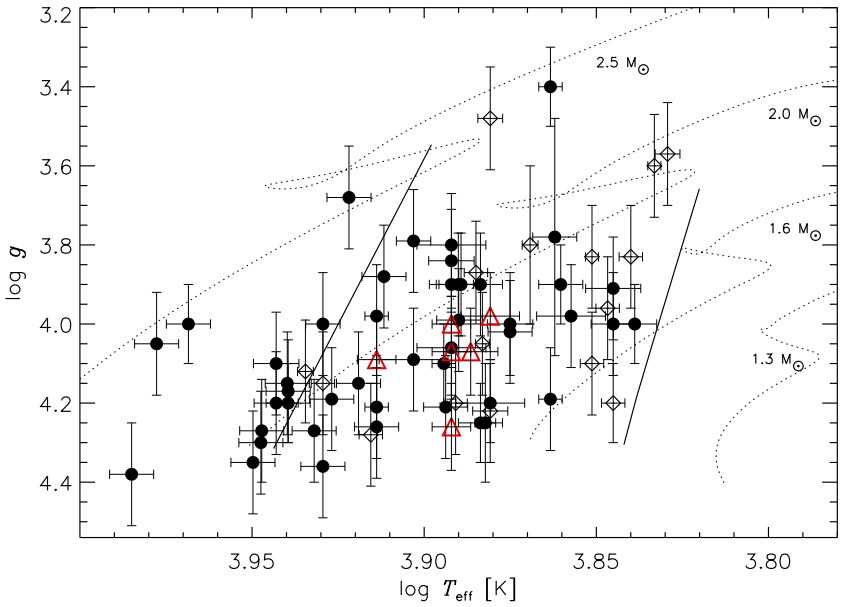

Figure 16. Positions of analysed and collected δ Sct stars in eclipsing binary systems. The symbols are the same as in Fig. 7. Solid lines represent the theoretical instability strips of δ Sct stars (Dupret et al. 2005). Triangle and square symbols illustrate the stars analysed spectroscopically in this study and the stars have $P_{\rm orb} > 13$ d, respectively. The evolutionary tracks were taken from Kahraman Aliçavuş et al. (2016).

correlation. Additionally, we found that the strength of F applied by the secondary component to the primary pulsation star affects $P_{\rm puls}$ and *Amp* in a negative way. The same correlation between F and $P_{\rm puls}$ was also obtained by Soydugan et al. (2006a).

5.3 Positions in HR diagram

The positions of the analysed primary δ Sct components in this study and the other primary δ Sct components given in the updated list in the Hertzsprung–Russell (HR) diagram are shown in Fig. 16. Our analysed δ Sct components and the δ Sct components given in the revised list are located in the δ Sct instability strip. However, there are a few stars (RR Lep, V2365 Oph, VV UMa, and V346 Cyg) placed beyond the blue edge of δ Sct instability strip. The $T_{\rm eff}$ and $\log g$ values of these stars were taken from literature spectral classification and photometric analyses (see Table A1 for references). Therefore, these stars should be re-analysed with new data.

In our study, the primary δ Sct components in eclipsing binaries were mostly located inside the theoretical δ Sct instability strip to within the error bars. However, in the study of Liakos & Niarchos (2017), there are more stars located beyond the blue border of δ Sct instability strip compared to our results. Liakos & Niarchos (2017) showed positions of δ Sct stars in all binaries, whereas we showed only the positions of δ Sct in eclipsing binaries. The fundamental parameters of stars can be obtained more accurately in the eclipsing binary case. Probably because of this reason Liakos & Niarchos (2017) found more stars located beyond the blue edge of δ Sct instability strip.

6 CONCLUSIONS

In this study, we present an updated list of δ Sct stars in eclipsing binaries and the spectroscopic analysis of six of δ Sct components in eclipsing binary systems.

In the spectroscopic analysis of six primary δ Sct components in eclipsing binaries, we obtained the spectral classification, $T_{\rm eff}$, $v \sin i$ and $[m/H]$ of the stars. XX Cep was found to be metal-rich, while others have approximately solar metallicity.

In the updated list of δ Sct components in eclipsing binaries, we collected the atmospheric and orbital parameters of the primary δ Sct components. We examined the properties of the primary δ Sct components and compared them with the properties of single δ Sct stars. Liakos & Niarchos (2017) stated that the single and binary member δ Sct stars have similar pulsational behaviour. However, when $P_{\rm puls}$ and V-band *Amp* of single and eclipsing binary member δ Sct stars were compared, we found that eclipsing binary member δ Sct stars oscillate with shorter $P_{\rm puls}$ and lower *Amp* comparing to single ones. These differences in pulsation quantities of single and binary δ Sct stars are thought to be caused by the effects of gravitational force applied by the secondary component on the primary and mass-transfer in these binaries. Additionally, binarity effects were also found when $P_{\rm puls}$ of detached and semidetached member δ Sct stars were compared. We showed that δ Sct stars in detached systems pulsate in longer periods.

The $v \sin i$ of single and eclipsing binary member δ Sct stars was also compared. We found that, on average, single δ Sct stars rotate faster than those in eclipsing binary systems.

We examined the relations between the orbital and atmospheric parameters of primary δ Sct components. First, the known $P_{\rm puls}$–$P_{\rm orb}$ correlation was checked and we obtained that $P_{\rm puls}$ increases with increasing $P_{\rm orb}$. Liakos & Niarchos (2017) found that binarity does not have a significant effect on pulsation if $P_{\rm orb} \geq 13$ d. However, we showed that the $P_{\rm puls}$–$P_{\rm orb}$ correlation is still significant even if $P_{\rm orb}$ is 26 d. Therefore, it appears that the 13-d limit for the binarity effect is too low. When our $P_{\rm puls}$–$P_{\rm orb}$ correlation was compared with the previously found correlations, we obtained similar trends except for the theoretically calculated relationship of Zhang et al. (2013). The difference between the theoretical relation and our correlation is caused by some parameters (f, q) having adverse effects on pulsation, whereas these parameters were found to be

directly proportional to pulsation in the theory. We also found that *V*-band *Amp* of primary δ Sct components increases with increasing $P_{\rm orb}$.

Significant negative relations between $P_{\rm puls}$ and atmospheric parameters $T_{\rm eff}$ and $\log g$ were found. The $\log g$–$\log P_{\rm puls}$ correlation was already known; however, the $P_{\rm puls}$–$T_{\rm eff}$ correlation for the primary δ Sct components was shown the first time. The $\log g$–$\log P_{\rm puls}$ correlation was compared with those in the literature. We find that our correlation is almost in agreement with that found for single δ Sct stars. However, the correlation found by Liakos & Niarchos (2017) is incompatible with ours.

A positive R–$\log P_{\rm puls}$ and a negative M–$\log P_{\rm puls}$ correlations were found. As both parameters influence the pulsation, we gave a new equation for $P_{\rm puls}$ in terms of R and M (equation 5). Additionally, we showed that increasing q caused increasing in $P_{\rm puls}$ for detached systems, while q has no effect on $P_{\rm puls}$ in semidetached systems. According to theory, $P_{\rm puls}$ should be directly proportional to q. The relationship between $P_{\rm puls}$ and $v \sin i$ of primary δ Sct components was also examined. No relationship was obtained for semidetached systems. However, for detached systems, $P_{\rm puls}$ of the primary δ Sct components decreases with increasing $v \sin i$. The suggested positive f and $P_{\rm puls}$ correlation by Zhang et al. (2013) was also checked. However, we found that $P_{\rm puls}$ is inversely proportional to f. When the relationship between $P_{\rm orb}$ and f was checked, we also obtained a negative correlation. Components in binaries come closer to each other with decreasing $P_{\rm orb}$ and the Roche lobes of the components become smaller; therefore f increases with decreasing $P_{\rm orb}$. This effect is rather dominant in binaries. Hence, we still see this effect in the f–$P_{\rm puls}$ relationship. Therefore, a negative correlation between these parameters was obtained contrary to suggested relation. Additionally, we found that the gravitational force applied by the secondary components on to the primary δ Sct components changes $P_{\rm puls}$ and *Amp* of δ Sct stars.

The positions of the primary δ Sct components in the $\log T_{\rm eff}$–$\log g$ diagram were shown. The primary δ Sct components in detached and semidetached systems are located inside the δ Sct instability strip. However, there are some semidetached member δ Sct components located beyond the blue edge of δ Sct instability strip, but the $T_{\rm eff}$ and $\log g$ of these stars may not be reliable.

In this study, we show the importance of δ Sct components in eclipsing binaries. The differences between the single and binary member δ Sct stars were emphasized. The effects of the fundamental and orbital parameters on pulsation and the correlations between the pulsation quantities and some fundamental parameters were given. These relationships allow us to infer the initial values of the fundamental parameters of pulsating δ Sct components. This is important for the theoretical examination of pulsating stars and understanding the internal structures and evolutionary statuses of stars. Additionally, utilizing the found $P_{\rm puls}$–$P_{\rm orb}$ correlation, the lower frequencies in δ Sct stars can be examined to see if they are related to binarity.

ACKNOWLEDGEMENTS

The authors would like to thank the reviewer for useful comments and suggestions that helped to improve the publication. This work has been partly supported by the Scientific and Technological Research Council of Turkey (TUBITAK) grant numbers 2214-A and 2211-C. We thank Çanakkale Onsekiz Mart University Research Foundation (Project no. FDK-2016-861) for supporting this study. This paper is a part of the PhD thesis of FKA. JK thanks to the grant 16-01116S (GAČR). We thank Dr G. Catanzaro for putting the code for Balmer lines analysis at our disposal. We are grateful to Dr D. Shulyak for putting the code for calculating $E(B-V)$ at our disposal. We thank Dr J. Ostrowski for helping us for the evolution tracks. This work has made use of data from the European Space Agency (ESA) mission *Gaia* (http://www.cosmos.esa.int/gaia), processed by the *Gaia* Data Processing and Analysis Consortium (DPAC, http://www.cosmos.esa.int/web/gaia/dpac/consortium). Funding for the DPAC has been provided by national institutions, in particular the institutions participating in the *Gaia* Multilateral Agreement. This research has made use of the SIMBAD data base, operated at CDS, Strasbourq, France.

REFERENCES

Aerts C., Christensen-Dalsgaard J., Kurtz D. W., 2010, Astroseismology. Springer-Verlag, Berlin
Alecian E., Catala C., van't Veer-Menneret C., Goupil M.-J., Balona L., 2005, A&A, 442, 993
Alfonso-Garzón J., Montesinos B., Moya A., Mas-Hesse J. M., Martín-Ruiz S., 2014, MNRAS, 443, 3022
Amôres E. B., Lépine J. R. D., 2005, AJ, 130, 659
Balona L. A., Dziembowski W. A., 2011, MNRAS, 417, 591
Bohm T., Zima W., Catala C., Alecian E., Pollard K., Wright D., 2008, Commun. Asteroseismol., 157, 47
Boksenberg A. et al., 1973, MNRAS, 163, 291
Breger M., 2000, in Breger M., Montgomery M., eds, ASP Conf. Ser. Vol. 210, Delta Scuti and Related Stars. Astron. Soc. Pac., San Francisco, p. 3
Budding E., Butland R., 2011, MNRAS, 418, 1764
Budding E., Erdem A., Çiçek C., Bulut I., Soydugan F., Soydugan E., Bakiş V., Demircan O., 2004, A&A, 417, 263
Casertano S., Riess A. G., Bucciarelli B., Lattanzi M. G., 2017, A&A, 599, A67
Catanzaro G., Leone F., Dall T. H., 2004, A&A, 425, 641
Chang S.-W., Protopapas P., Kim D.-W., Byun Y.-I., 2013, AJ, 145, 132
Chapellier E. et al., 2004, A&A, 426, 247
Christiansen J. L., Derekas A., Ashley M. C. B., Webb J. K., Hidas M. G., Hamacher D. W., Kiss L. L., 2007, MNRAS, 382, 239
Claret A., Rodriguez E., Rolland A., Lopez de Coca P., 1990, in Cacciari C., Clementini G., eds, ASP Conf. Ser. Vol. 11, Confrontation Between Stellar Pulsation and Evolution. Astron. Soc. Pac., San Francisco, p. 481
Cox J. P., 1980, Theory of Stellar Pulsation. Princeton Univ. Press, Princeton, NJ
Creevey O. L. et al., 2009, A&A, 507, 901
Creevey O. L. et al., 2010, Astron. Nachr., 331, 952
da Silva R., Maceroni C., Gandolfi D., Lehmann H., Hatzes A. P., 2014, A&A, 565, A55
Dal H. A., Sipahi E., 2013, Publ. Astron. Soc. Aust., 30, e016
Dimitrov D., Kraicheva Z., Popov V., 2008, Inf. Bull. Var. Stars, 5856, 1
Dimitrov D., Kraicheva Z., Popov V., 2009a, Inf. Bull. Var. Stars, 5883, 1
Dimitrov D., Kraicheva Z., Popov V., 2009b, Inf. Bull. Var. Stars, 5892, 1
Droege T. F., Richmond M. W., Sallman M. P., Creager R. P., 2006, PASP, 118, 1666
Dupret M.-A., Grigahcène A., Garrido R., Gabriel M., Scuflaire R., 2005, A&A, 435, 927
Dvorak S., 2009, Commun. Asteroseismol., 160, 64
Erdem A., Öztürk O., 2016, New Astron., 48, 33
ESA, 1997, VizieR Online Data Catalog, 1239
Escolà-Sirisi E., Juan-Samsó J., Vidal-Sáinz J., Lampens P., García-Melendo E., Gómez-Forrellad J. M., Wils P., 2005, A&A, 434, 1063
Fernie J. D., 1965, ApJ, 142, 1072
Gaulme P., Guzik J. A., 2014, in Guzik J. A., Chaplin W. J., Handler G., Pigulski A., eds, Proc. IAU Symp. 301, Precision Asteroseismology. Cambridge Univ. Press, Cambridge, p. 413
Gray D. F., 2008, The Observation and Analysis of Stellar Photospheres. Cambridge Univ. Press, Cambridge

Gray R. O., Corbally C. J., Garrison R. F., McFadden M. T., Robinson P. E., 2003, AJ, 126, 2048
Griffin R. F., Boffin H. M. J., 2003, The Observatory, 123, 203
Gunsriwiwat K., Mkrtichian D. E., 2015, Inf. Bull. Var. Stars, 6148, 1
Guo Z., Gies D. R., Matson R. A., García Hernández A., 2016, ApJ, 826, 69
Hambálek Ľ., 2015, Contrib. Astron. Obs. Skalnaté Pleso, 45, 106
Hambleton K. M. et al., 2013, MNRAS, 434, 925
Hambsch F.-J., Lampens P., van Cauteren P., Kleidis S., Robertson C. W., Krajci T., Wils P., 2010, Inf. Bull. Var. Stars, 5949, 1
Heckmann O., 1975, in Dieckvoss W., ed., AGK 3. Star Catalogue of Positions and Proper Motions North of −2.5 deg. Declination. Hamburg-Bergedorf: Hamburger Sternwarte.
Heckmann O., 1975, Hamburg-Bergedorf: Hamburger Sternwarte.
Heiter U. et al., 2002, A&A, 392, 619
Herbig G. H., 1960, ApJ, 131, 632
Hong K., Lee J. W., Kim S.-L., Koo J.-R., Lee C.-U., Yushchenko A. V., Kang Y.-W., 2015, AJ, 150, 131
Hosseinzadeh B., Pazhouhesh R., Yakut K., 2014, New Astron., 27, 95
Houdek G., Balmforth N. J., Christensen-Dalsgaard J., Gough D. O., 1999, A&A, 351, 582
Howarth I. D., 1983, MNRAS, 203, 301
Høg E. et al., 1997, A&A, 323, L57
Ibanoğlu C. et al., 2008, MNRAS, 384, 331
Kacar Y., 2012, PhD thesis, Canakkale Onsekiz Mart University
Kahraman Aliçavuş F. et al., 2016, MNRAS, 458, 2307
Khaliullin K. F., Kozyreva V. S., 1989, Ap&SS, 155, 53
Kim S.-L., Lee J. W., Youn J.-H., Kwon S.-G., Kim C., 2002, A&A, 391, 213
Kim S.-L., Lee J. W., Kwon S.-G., Youn J.-H., Mkrtichian D. E., Kim C., 2003, A&A, 405, 231
Kim S.-L., Kwon S.-G., Lee D. J., Lee C.-U., Jin H., Lee J. W., 2004, in Kurtz D. W., Pollard K. R., eds, ASP Conf. Ser. Vol. 310, IAU Colloq.193: Variable Stars in the Local Group. Astron. Soc. Pac., San Francisco, p. 399
Kim S.-L., Lee C.-U., Lee J. W., 2006, Mem. Soc. Astron. Ital., 77, 184
Kim S.-L., Lee J. W., Lee C.-U., Youn J.-H., 2010, PASP, 122, 1311
Koo J.-R., Lee J. W., Hong K., Kim S.-L., Lee C.-U., 2016, AJ, 151, 77
Korda D., Zasche P., Kučáková H., 2015, New Astron., 40, 64
Kundra E., Hric L., Gális R., 2013, Balt. Astron., 22, 111
Kurtz D. W., Hambleton K. M., Shibahashi H., Murphy S. J., Prša A., 2015, MNRAS, 446, 1223
Kurucz R., 1993, ATLAS9 Stellar Atmosphere Programs and 2 km/s grid. Kurucz CD-ROM No. 13. Cambridge, Mass.: Smithsonian Astrophysical Observatory, 1993, 13
Kurucz R. L., Avrett E. H., SAO Special Report 391
Lampens P., 2006, in Sterken C., Aerts C., eds, ASP Conf. Ser. Vol. 349, Astrophysics of Variable Stars. Astron. Soc. Pac., San Francisco, p. 153
Lampens P., van Cauteren P., Strigachev A., Kim S.-L., Kang Y. B., Koo J.-R., Mkrtichian D. E., 2004, Inf. Bull. Var. Stars, 5572, 1
Lázaro C., Arévalo M. J., Claret A., Rodríguez E., Olivares I., 2001, MNRAS, 325, 617
Lee J. W., Kim S.-L., Hong K., Koo J.-R., Lee C.-U., Youn J.-H., 2016a, AJ, 151, 25
Lee J. W., Hong K., Kim S.-L., Koo J.-R., 2016b, MNRAS, 460, 4220
Lehmann H., Southworth J., Tkachenko A., Pavlovski K., 2013, A&A, 557, A79
Liakos A., Cagaš P., 2014, Ap&SS, 353, 559
Liakos A., Niarchos P., 2012, New Astron., 17, 634
Liakos A., Niarchos P., 2013, Ap&SS, 343, 123
Liakos A., Niarchos P., 2015, in Rucinski S. M., Torres G., Zejda M., eds, ASP Conf. Ser. Vol. 496, Living Together: Planets, Host Stars and Binaries. Astron. Soc. Pac., San Francisco, p. 195
Liakos A., Niarchos P., 2016, preprint (arXiv:1606.08638)
Liakos A., Niarchos P., 2017, MNRAS, 465, 1181
Liakos A., Ulas B., Gazeas K., Niarchos P., 2008, Commun. Asteroseismol., 157, 336
Liakos A., Zasche P., Niarchos P., 2010, in Prša A., Zejda M., eds, ASP Conf. Ser. Vol. 435, Binaries - Key to Comprehension of the Universe. Astron. Soc. Pac., San Francisco, p. 101
Liakos A., Niarchos P., Soydugan E., Zasche P., 2012, MNRAS, 422, 1250
Liu N., Zhang X.-B., Ren A.-B., Deng L.-C., Luo Z.-Q., 2012, Res. Astron. Astrophys., 12, 671
Maceroni C. et al., 2014, A&A, 563, A59
Manimanis V. N., Vamvatira-Nakou C., Niarchos P. G., 2009, Ap&SS, 323, 115
Manzoori D., Salar A., 2016, AJ, 152, 26
Mason B. D., Hartkopf W. I., Gies D. R., Henry T. J., Helsel J. W., 2009, AJ, 137, 3358
Mkrtichian D. E., Gamarova A. Y., 2000, Inf. Bull. Var. Stars, 4836, 1
Mkrtichian D. E. et al., 2004, A&A, 419, 1015
Monet D. G. et al., 2003, AJ, 125, 984
Moriarty D. J. W., Bohlsen T., Heathcote B., Richards T., Streamer M., 2013, J. Am. Assoc. Var. Star Obs., 41, 182
Narusawa S.-y., 2013, PASJ, 65, 105
Niemczura E., Smalley B., Pych W., 2014, Determination of Atmopsheric Parameters of B-, A-, F- and G-Type Stars Lectures from the School of Spectroscopic Data Analyses. Springer-Verlag, Berlin
Norton A. J., Lohr M. E., Smalley B., Wheatley P. J., West R. G., 2016, A&A, 587, A54
Pigulski A., Michalska G., 2007, Acta Astron., 57, 61
Piskunov N. E., Kupka F., Ryabchikova T. A., Weiss W. W., Jeffery C. S., 1995, A&AS, 112, 525
Popper D. M., 1988, AJ, 95, 190
Rodríguez E., López-González M. J., López de Coca P., 2000, A&AS, 144, 469 (R2000)
Rodríguez E. et al., 2010, MNRAS, 408, 2149
Russo G., Milano L., 1983, A&AS, 52, 311
Sana H., Evans C. J., 2011, in Neiner C., Wade G., Meynet G., Peters G., eds, Proc. IAU Symp. 272, Active OB Stars: Structure, Evolution, Mass Loss, and Critical Limits. Cambridge Univ. Press, Cambridge, p. 474
Schmid V. S. et al., 2015, A&A, 584, A35
Seaton M. J., 1979, MNRAS, 187, 73
Senyüz T., Soydugan E., 2008, Commun. Asteroseismol., 157, 365
Shibahashi H., Kurtz D. W., 2012, MNRAS, 422, 738
Skrutskie M. F. et al., 2006, AJ, 131, 1163
Šlechta M., Škoda P., 2002, Publ. Astron. Inst. Acad. Sci. Czech Rep., 90, 9
Soufi F., Goupil M. J., Dziembowski W. A., 1998, A&A, 334, 911
Southworth J. et al., 2011, MNRAS, 414, 2413
Soydugan E., Kaçar Y., 2013, AJ, 145, 87
Soydugan E., Soydugan F., 2007, in Demircan O., Selam S. O., Albayrak B., eds, ASP Conf. Ser. Vol. 370, Solar and Stellar Physics Through Eclipses. Astron. Soc. Pac., San Francisco, p. 344
Soydugan E., DemİrcanO., Akan M. C., Soydugan F., 2003, AJ, 126, 1933
Soydugan E., İbanoğlu C., Soydugan F., Akan M. C., Demircan O., 2006a, MNRAS, 366, 1289
Soydugan E., Soydugan F., Demircan O., İbanoğlu C., 2006b, MNRAS, 370, 2013
Soydugan E., Soydugan F., Şenyüz T., Püsküllü Ç., Demircan O., 2011, New Astron., 16, 72
Soydugan F., Soydugan E., Kanvermez Ç., Liakos A., 2013, MNRAS, 432, 3278
Soydugan E., Soydugan F., Aliçavuş F., Erdem A., 2016, New Astron., 46, 40
Tkachenko A., Lehmann H., Mkrtichian D. E., 2009, A&A, 504, 991
Tkachenko A., Lehmann H., Mkrtichian D., 2010, AJ, 139, 1327
Tkachenko A. et al., 2013, A&A, 556, A52
Turcu V., Pop A., Moldovan D., 2008, Inf. Bull. Var. Stars, 5826, 1
Turcu V., Pop A., Marcu A., Moldovan D., 2011, Ap&SS, 331, 105
Uytterhoeven K. et al., 2011, A&A, 534, A125
Valenti J. A., Piskunov N., 1996, A&AS, 118, 595
Van Eylen V., Winn J. N., Albrecht S., 2016, ApJ, 824, 15
van Leeuwen F., 2007, A&A, 474, 653
Yang Y.-G., Wei J.-Y., Li H.-L., 2014, AJ, 147, 35

Zasche P., 2011, New Astron., 16, 157
Zhang X. B., 2008, in Deng L., Chan K.-L., eds, Proc. IAU Symp. 252, The Art of Modeling Stars in the 21st Century. Cambridge Univ. Press, Cambridge, p. 429
Zhang X. B., Luo C. Q., Fu J. N., 2013, ApJ, 777, 77
Zhang X. B. et al., 2014, AJ, 148, 106
Zhang X. B., Luo Y. P., Wang K., 2015a, AJ, 149, 96
Zhang X. B., Luo Y. P., Wang K., Luo C. Q., 2015b, AJ, 150, 37
Zhou A.-Y., 2001, Inf. Bull. Var. Stars, 5087, 1
Zwitter T., Munari U., Marrese P. M., Prša A., Milone E. F., Boschi F., Tomov T., Siviero A., 2003, A&A, 404, 333

APPENDIX

Table A1. The list of *δ* Sct stars in eclipsing binaries. The fundamental, orbital and atmospheric parameters of primary *δ* Sct and secondary components. The subscripts p and s represent primary and secondary components, respectively.

HD	Name	V (mag)	Spectral type	Parallaxes (mas)	Type	$P_{\rm orb}$ (d)	$P_{\rm puls}$ (d)	Amp$_V$ (mmag)	Amp$_B$ (mmag)	$T_{{\rm eff}p}$ (K)	$T_{{\rm eff}s}$ (K)	log g_p	$v \sin i_p$ (km s^{-1})
354963	QY Aql	11.89	F0	1.74 (87)	SD	7.2296	0.0938	9.4 (2)	11.8 (2)	7300	4244 (122)	3.4 (10)	
193740	XZ Aql	10.18	A2/3 II/III	2.03 (44)	SD	2.1392	0.0326	6.8 (2)	8.6 (2)	8770 (150)	4720 (150)	4.10 (03)	
	V729 Aql	13.76			SD	1.2819	0.0357	4.2 (4)		6900	4300 (175)	4.00 (10)	
	V1464 Aql	08.68	A2V	4.12 (48)	SD	0.6978	0.0171	24.0 (3)	30.0 (2)	7420 (192)	6232 (161)		
	CZ Aqr	11.10	A5		SD	0.8627	0.0282		3.7 (5)	8200	5650 (12)	4.21	42
211705	DY Aqr	10.49	A1/2 III	1.83 (75)	SD	2.1597	0.0428	9.4		7625 (125)	3800 (200)	4.25 (25)	50 (10)
203069	RY Aqr	9.25	A7V	6.48 (28)	SD					7650	4520 (122)	4.25 (60)	
	V551 Aur	14.27	F		D	1.1732	0.1294	19.1 (3)	15.7 (3)	7000	6085 (34)		
	EW Boo	10.26	A0	2.23 (26)	SD	0.9063	0.0191	12.4 (2)	14.4 (2)	7840	4515 (35)	4.1 (10)	
	YY Boo	11.58	A4+K4IV	1.17 (23)	SD	3.9330	0.0613	79.2 (2)	116.8(2)		4650 (10)		
	Y Cam	10.60	A9IV+K1IV	0.82 (30)	SD	3.3058	0.0665	12.2		8000 (250)	4629 (150)	3.79	51 (4)
194168	TY Cap	10.36	A5 III	1.95 (55)	SD	1.4235	0.0413	15.6 (7)	18.5 (7)	8200	4194 (30)	3.98	
	AB Cas	10.32	A3 V	2.91 (22)	SD	1.3669	0.0583	19.6 (9)	22.2 (1)	8000	4729 (24)		
	IV Cas	11.34	A2	1.06 (40)	SD	0.9985	0.0306		3.4 (2)	8500 (250)	5193 (7)	4.0 (50)	115 (5)
017138	RZ Cas	6.26	A3 V	14.99 (34)	SD	1.1952	0.0156	5.4 (3)	2.7 (3)	8907 (15)	4797 (20)	4.35	66 (1)
	V389 Cas	11.09			D	2.4948	0.0370	9.2 (4)		7673 (31)	4438 (22)	3.87	
	V1264 Cen	11.95	A7V	0.97 (39)	SD	5.3505	0.0734	350.0		7500	4200	4.00	
222217	XX Cep	9.18	A7V	3.17 (23)	SD	2.3374	0.0310	2.6 (2)	2.9 (2)	8000 (250)	4280 (36)	4.09	50
	WY Cet	9.28	F0V	4.64 (73)	SD	1.9396	0.0757		7.7 (3)	7500	4347 (7)	4.02	
075747	RS Cha	6.07	A7V		D	1.6699	0.0473			7640 (76)	7230 (72)	4.05	64 (6)
057167	R Cma	5.70	F2 III/IV	23.3 (59)	SD	1.1359	0.0471			7300	4350	4.19	82 (3)
	UW Cyg	10.86	A7/A6 IV	1.60 (30)	SD	3.4507	0.0359		1.9 (2)	7800 (250)	4347 (4)	4.06	45
	V346 Cyg	12.22	A5	1.11 (22)	SD	2.7433	0.0502		30.00	8353	6620	3.68	
	V469 Cyg	12.33	B8+F0		SD	1.3124	0.0278	20.0				4.13	
099612	AK Crt	11.28	A5/9 II/III	1.81 (48)	D	2.7788	0.0680	8-35					
	BW Del	11.28	F2		SD	2.4231	0.0398	1.8 (2)	2.9 (2)	7000	4061 (30)	4.00	
152028	GK Dra	8.77	F0	3.03 (22)	D	16.960	0.1138			7100 (70)	6878 (57)	3.83 (03)	
	GQ Dra				SD	0.7659	0.0335						
172022	HL Dra	7.36	A6IV	6.24 (24)	SD	0.9443	0.0372	2.8 (3)	3.0 (2)	7800 (250)	5074 (8)	3.80	88
173977	HN Dra	8.07	F2	3.88 (23)	D	1.8008	0.1169	7.6		6918	6309	3.83	73
187708	HZ Dra	8.14	A8/A7 V	4.89 (29)	D	0.7729	0.0196		4.0 (4)	7600 (250)	5015 (68)	4.22	120
	OO Dra	11.39		1.54 (29)	D	1.2384	0.0239	4.2 (2)	4.9 (3)	8500	6452 (8)	4.15	
238811	SX Dra	10.40	A7V+ K7IV	1.16 (27)	SD	5.1696	0.0440	23.6 (3)	34.6 (4)	7762	4638 (200)	3.99	
139319	TW Dra	7.46	A5+K0III	5.90 (24)	SD	2.8069	0.0530		10.00	8160 (15)	4538 (11)	3.88 (02)	47 (1)
	TZ Dra	9.32	A7V	3.96 (25)	SD	0.8660	0.0196	2.8 (2)	3.7 (2)	7600 (250)	5088 (55)	4.20 (10)	80
021985	AS Eri	8.30	A1V	5.06 (51)	SD	2.6641	0.0169			8500	4790	4.35	40
	TZ Eri	9.61	A5	3.27 (34)	SD	2.6061	0.0534	7.3	8.30	9307 (20)	4562		
336759	BO Her	11.14	A7	1.51 (30)	SD	4.2728	0.0745	50.8 (3)	68.0 (3)	7800	4344 (68)	3.90 (10)	
	CT Her	11.32	A3V	0.83 (46)	SD	1.7864	0.0189		3.3 (1)	8700	4651 (7)	4.17 (02)	50
	EF Her	11.53	A0	1.14 (26)	SD	4.7292	0.0310	51.0	69.0	9327	4767		
151973	LT Her	10.55	A1	1.71 (81)	SD					9400	5063 (25)		
	TU Her	11.14	A5	1.84 (22)	SD	2.2669	0.0556	9-10					
	V948 Her	8.91	F2	6.15 (26)	D	2.0831	0.0947	31.0		7000	4310 (63)	4.20 (10)	
	AI Hya	9.35	F2m+F0V	1.88 (35)	D	8.2897	0.1380	20.0		7100	6750	4.10	
078014	RX Hya	9.56	A5 III	3.80 (33)	SD	2.2817	0.0516	7.0					
	AU Lac	11.81	A5	1.60 (20)	SD	1.3926	0.0172		5.00	8200	3784 (15)	4.26	
	WY Leo	10.89	A2	1.51 (49)	SD	4.9858	0.0656	11.0 (1)				3.79	
	Y Leo	10.07	A3V	2.50 (26)	SD	1.6861	0.0290	8.12 (15)		8855	4276 (23)	4.27	
033789	RR Lep	10.14	A4 III	2.20 (35)	SD	0.9154	0.0300	7.6 (4)	9.6 (4)	9300	4904 (106)	4.00 (10)	
	CL Lyn	9.77	A8 IV	2.82 (25)	SD	1.5861	0.0434	5.7 (4)	7.3 (3)	7200 (250)	4948 (14)	3.98	75
198103	VY Mic	9.54	A4 III/IV	1.66 (36)	SD	4.4364	0.0817	19.4 (2)		8705	5301	4.15	
	V577 Oph	11.19	A	1.29 (26)	D	6.0791	0.0695	57.8					
155002	V2365 Oph	8.86	A2	3.54 (29)	SD	4.8656	0.0700	50.0		9500	6400 (27)	4.05	

Table A1. *– continued*

HD	Name	V (mag)	Spectral type	Parallaxes (mas)	Type	$P_{\rm orb}$ (d)	$P_{\rm puls}$ (d)	Amp$_V$ (mmag)	Amp$_B$ (mmag)	$T_{{\rm eff}p}$ (K)	$T_{{\rm eff}s}$ (K)	log g_p	$v \sin i_p$ (km s^{-1})
293808	FL Ori	11.42	A2	2.05 (40)	D	1.5510	0.0550			8232	5243	4.28	
248406	FR Ori	10.64	A7	2.53 (86)	SD	0.8832	0.0259	5.8		7830	4583 (10)	4.21	
252973	V392 Ori	10.49	A5V	2.56 (25)	SD	0.6593	0.0246			8300	5065 (11)	4.15	
	MX Pav	11.35	A5+K3IV	1.56 (38)	SD	5.7308	0.0756	76.9 (3)					
	BG Peg	11.35	A2		SD	1.9527	0.0391	30.6 (5)	36 (6)	8770	5155 (200)	4.20	
275604	AB Per	9.72	F0		SD	7.1603	0.1954						
	IU Per	10.56	A4	1.62 (45)	SD	0.8570	0.0232	3.08 (07)		8450	4900 (250)	4.29	
	AO Ser	11.04	A2	2.19 (41)	SD	0.8793	0.0465		20.00	8860	4547 (512)	4.30	
	UZ Sge	11.40	A0		SD	2.2157	0.0214			8700	4586 (60)	4.20 (10)	
	AC Tau	11.09	A8	1.65 (43)	SD	2.0434	0.0570	6.0					
	IZ Tel	12.20	A8+G8 IV	0.52 (26)	SD	4.8802	0.0738	45.9 (4)					
12211	X Tri	9.00	A7V	4.85 (22)	SD	0.9715	0.0220	20.0		8600	5188 (4)		
115268	IO UMa	8.21	A3	1.05 (43)	SD	5.5202	0.0454	10 (2)	13.0 (2)	7800 (150)	4260 (30)	3.84 (05)	35 (2)
	VV UMa	10.28	A2V	2.45 (45)	SD	0.6874	0.0205	28.0 (1)		9660 (30)	5579 (20)	4.38	
	AW Vel	10.70	A7	1.69 (41)	SD	1.9925	0.0658	58.0 (1)					
	BF Vel	10.62	A3	1.92 (30)	SD	0.7040	0.0223		26.0 (2)	8550	4955 (4)	4.27	
	CoRot 105906206	12.21		0.96 (25)	D	3.6946	0.1062			6750 (150)	6152 (162)	3.57	48 (1)
172189	GSC 455-1084	8.73	A6V-A7V		D	5.7017	0.0510			7600 (150)	8100 (150)	3.48	78 (3)
232486	GSC 3671-1094	9.64	A5	3.07 (25)	D	2.3723	0.0409	20.0					
	GSC 3889-202	10.39	A7 V-IV	1.27 (24)	SD	2.7107	0.0441	50.0	70.0	7750	4500	3.90	60
	GSC 4293-432	10.56	A7+K3		SD	4.3844	0.1250	35.0	40.0	7750	4300		40
	GSC 4588-883	11.31	A9 IV+K4III	0.94 (48)	SD	3.2586	0.0493			7650	4100	3.90	60
062571	GSC 4843-2140	8.83	F0-F2		SD	3.2087	0.1141	41.7		7762	5719 (150)		
220687	GSC 5825-1038	9.60	A2 III	2.31 (42)	D	1.5943	0.0382	12.8 (14)					
	KIC 3858884	9.28	F5	1.78 (22)	D	25.952	0.1383			6810 (70)	6890 (80)	3.60	32 (2)
181469	KIC 4150611	08.00	A2	7.73 (46)	D	94.090				7400 (100)		3.80 (20)	128 (5)
	KIC 4544587	10.83		1.36 (41)	D	2.1891	0.0208			8600 (100)	7750 (180)	4.12 (02)	87 (13)
	KIC 4739791	14.63	A7V		D	0.8989	0.0482			7778 (28)	5447 (17)	4.20 (02)	
	KIC 6220497				SD	1.3232	0.1174			7279 (54)	3907 (22)	3.78 (30)	
	KIC 6629588				D	2.2645	0.0746			6787 (247)	4405 (621)		
	KIC 8569819				D	20.849				7100 (250)	6047 (253)		
	KIC 9851944	11.42			D	2.1639	0.0962			7026 (50)	6950 (50)	3.96	53 (7)
	KIC 10619109	11.90			SD	2.0452	0.0234			7138 (284)	3824 (571)		
	KIC 10661783	9.53	A2	1.94 (26)	SD	1.2314	0.0355			7764 (54)	5980 (72)	3.90	79 (4)
	KIC 10686876	11.54	F0V		D	2.6184	0.0476			8167 (285)	6475 (817)		
	KIC 11175495				SD	2.1911	0.0155			8293 (290)	6999 (790)		
	KIC 11401845				D	2.2000				7590			
	TYC 7053-566-1	11.51		1.09 (23)	SD	5.1042	0.0743			7000 (200)	4304 (9)	3.91 (02)	
	USNO-A2.0 1200-03937339	14.53			SD	1.1796	0.0326	5.1 (4)		7250	4320 (108)	3.90 (10)	

Table A1. – *continued*

HD	Name	i (^{0})	q	f	M_p ($M_\odot$)	M_s ($M_\odot$)	R_p ($R_\odot$)	R_s ($M_\odot$)	L_p ($L_\odot$)	L_s ($L_\odot$)	$M_{bol,\,p}$ (mag)	$M_{bol,\,s}$ (mag)	a_p ($R_\odot$)	a_s ($R_\odot$)	References
354963	QY Aql	88.6 (5)	0.250 (200)	0.403	1.6 (2)	0.4 (1)	4.1 (2)	5.4 (2)	43.0 (3.0)	8.0 (1)			4.0 (2)	16.3 (7)	6, 43
193740	XZ Aql	84.8 (1)	0.204 (2)	0.500	2.5 (1)	0.5 (03)	2.3 (04)	2.5 (04)	6.0 (04)	0.5 (07)	1.1 (1)	3.6 (2)	10.1 (1)		6, 74
	V729 Aql	77.3 (2)	0.440 (10)	0.723	1.5 (2)	0.7 (1)	2.0 (01)	2.0 (01)	7.8 (1)	1.3 (2)	2.0 (1)	4.6 (1)			44
	V1464 Aql	38.4 (2)	0.710 (20)	1.000		2.1 (05)	1.8 (01)		12.0 (3)	4.4 (02)			4.8		6, 12, 85
	CZ Aqr	89.7 (1)	0.490 (100)	0.780	2.0	1.0 (1)	1.9 (1)	1.8 (1)	15.3 (9)	2.9 (2)	1.8 (6)	3.6 (6)	1.9 (2)	3.8 (1)	42
211705	DY Aqr	75.4 (5)	0.310 (200)	0.489	1.8 (2)	0.6 (4)	2.1 (1)	2.7 (1)					9.4 (5)	9.4 (5)	2, 6
203069	RY Aqr	83.2 (4)	0.204 (6)		1.3 (1)	0.3 (02)	1.4 (07)	1.9 (1)	56.0 (9)	1.4 (3)	4.4 (2)	2.8 (2)	7.6		6, 56
	V551 Aur	74.3 (1)	0.725 (6)	0.539											53
	EW Boo	76.5 (1)	0.130 (2)	0.708	1.8 (2)	0.2 (02)	1.8 (1)	1.1 (04)	10.9 (5)	0.4 (1)			5.0 (2)		6, 80, 85
	YY Boo	81.7 (1)	0.290 (10)	0.303											6, 25
	Y Cam	85.6 (1)	0.241	0.535	2.1 (1)	0.5	3.1 (05)	3.3 (05)	1.4 (06)	0.5 (06)	1.3 (2)	3.6 (2)			6, 26, 35, 42, 62, 85
194168	TY Cap	80.4 (2)	0.520 (100)	0.706	2.0 (1.1)	1.1	2.5 (1)	2.5 (1)	24.3 (8)	1.8 (2)	1.3 (1)	4.1 (1)	2.7 (3)	5.2 (1)	6, 42
	AB Cas	88.3 (1)	0.190	0.535											6, 68, 85
	IV Cas	87.5 (5)	0.408 (1)	0.781	2.0 (1)	0.8 (04)	2.1 (04)	1.8 (03)	1.3 (05)	0.3 (05)	1.4 (1)	3.9 (1)			6, 31, 32
017138	RZ Cas	82.0 (3)	0.342 (1)	0.494	2.0 (2)	0.7 (1)	1.6 (1)	1.9					6.6 (3)		6, 70, 75, 85
	V389 Cas	81.8 (2)			1.5 (01)	1.5 (01)	2.5 (02)	2.6 (05)		1.6	3.9 (1)	0.1			6, 38
	V1264 Cen	86.5 (1)	0.220 (20)	0.350	1.5 (02)	0.3 (02)	2.4 (02)	4.0 (01)	6.7 (03)	3.9 (03)	1.8	3.5			6, 8
222217	XX Cep	81.6 (1)	0.173 (5)	0.387	2.5 (1)	0.4 (01)	2.3 (02)	2.4 (02)	20.0 (3.0)	2.1 (4)	1.5 (2)	3.9 (4)			6, 27, 37, 85
	WY Cet	81.8 (1)	0.260 (10)	0.514	1.7	0.4 (01)	2.2 (1)	2.3 (1)	14.0 (9)	1.7 (1)	1.9 (8)	4.2 (8)	1.8 (3)	6.9 (1)	6, 42, 85
075747	RS Cha	83.4 (3)	0.709		1.9 (01)		1.9 (01)	2.2 (06)	2.4 (06)						1, 3, 85
057167	R Cma	81.7 (2)	0.140	0.542	1.7 (1)	0.2 (1)	1.8 (03)	1.2 (07)	8.2 (2)	0.5 (01)			5.7	5.7	4, 6, 57, 85
	UW Cyg	87.1 (1)	0.140 (100)	0.316	1.9	0.3 (1)	2.2 (1)	2.9 (1)	18.0 (9)	2.6 (1)	1.6 (4)	3.7 (6)	1.5 (2)	11.2 (1)	6, 42
	V346 Cyg				2.3	1.8	3.8	4.7	61.8	39.9					6, 69, 85
	V469 Cyg	81.0	0.430		3.3		2.7								5, 42, 69
099612	AK Crt														6, 61
	BW Del	78.6 (4)	0.160 (20)	0.416	1.5 (2)	0.3 (1)	2.1 (1)	2.2 (1)	10.0 (1)	1.2 (1)	1.3 (1)	8.0 (4)			43
152028	GK Dra	86.1 (2)	1.244 (20)	0.356	1.5 (1)	1.8 (1)	2.4 (04)	2.8 (05)			2.0 (1)	1.8 (1)			6, 20, 85, 89
	GQ Dra														51
172022	HL Dra	66.5 (1)	0.370 (100)	0.859	2.5 (2)	0.9 (1)	2.5 (4)	1.8 (3)	24.3 (7)	1.9 (1)	1.3 (2)	4.1 (2)	1.7 (3)	4.4 (1)	6, 42, 85
173977	HN Dra	67.0	0.931		1.9	1.3	2.9	1.4							6, 7, 85
187708	HZ Dra	72.0 (3)	0.120 (40)	0.773	3.0 (3)	0.4 (1)	2.3 (1)	0.8 (1)	45.0 (3.0)	0.4 (2)	0.6 (4)	5.9 (4)	0.6 (1)	4.7 (1)	6, 42, 85
	OO Dra	85.7 (1)	0.097 (2)	0.558	2.0 (3)	0.3 (03)	2.0 (1)	1.2 (05)							6, 87
238811	SX Dra	85.3 (1)	0.373 (2)	0.320	1.8	0.5	2.3	4.3	16.4						6, 73
139319	TW Dra	86.8 (3)	0.411 (4)	0.581	2.2 (1)	0.9 (05)	2.6 (02)				1.3 (1)	3.2	12.2 (2)		6, 34, 76, 85
	TZ Dra	77.6 (1)	0.310 (30)	0.665	1.8 (2)	0.6 (1)	1.7 (1)	1.5 (1)	9.0 (1.0)	1.3 (1)			1.2 (1)	4.0 (2)	6, 43
021985	AS Eri		0.277		1.9		1.6								6, 42, 59, 85
	TZ Eri	87.7 (07)	0.177 (5)	0.306											6, 40
336759	BO Her	85.4 (4)	0.220 (200)	0.324	1.8 (2)	0.4 (1)	2.5 (1)	3.8 (1)	20.0 (1.0)	4.6 (4)			2.7 (1)	12.1 (5)	6, 43
	CT Her	81.9 (01)	0.141	0.432	2.3 (02)	0.3 (04)	2.1 (06)	1.9 (08)	17.4 (2.4)	1.2 (2)	1.7 (2)	4.5 (2)			1, 6, 45
	EF Her	77.80	0.210	0.421											6, 65
151973	LT Her	75.6 (2)	0.200 (3)	0.840	2.5	0.5	2.7	1.6	49.5	1.7					6, 63
	TU Her														6, 46
	V948 Her	84.4 (6)	0.270 (30)	0.574	1.5 (2)	0.4 (07)	1.6 (1)	0.7 (3)	6.0 (1.0)	0.2 (1)	2.9 (2)	7.0 (1.0)	1.3 (7)	4.9 (2)	6, 41, 42
	AI Hya	89.9 (1)			1.9	2.1	2.1	3.8			1.5	1.2			6, 30, 62, 69

Table A1. – *continued*

HD	Name	i (^{0})	q	f	M_p ($M_\odot$)	M_s ($M_\odot$)	R_p ($R_\odot$)	R_s ($M_\odot$)	L_p ($L_\odot$)	L_s ($L_\odot$)	$M_{bol,\,p}$ (mag)	$M_{bol,\,s}$ (mag)	a_p ($R_\odot$)	a_s ($R_\odot$)	References
078014	RX Hya														6, 34, 85
	AU Lac	83.0 (1)	0.300 (10)	0.490	2.0	0.6 (1)	1.8 (1)	2.1 (1)	12.6 (7)	0.8 (1)	2.0 (6)	5.0 (7)	1.7 (2)	5.7 (1)	6, 42, 59
	WY Leo					2.3	3.3								5, 6, 16
	Y Leo	86.1 (2)	0.324 (3)		2.3	0.7	1.9	2.5					8.6		6, 76, 77, 85
033789	RR Lep	80.5 (6)	0.287 (21)	0.802	2.5 (3)	0.7 (1)	2.4 (1)	1.5 (2)	15.6 (4)	1.0 (1)	0.8 (4)	4.6 (8)	5.1 (1)	5.9 (1)	6, 17, 43
	CL Lyn	78.7 (1)	0.190 (20)	0.606	2.0	0.4	2.5 (1)	1.9 (1)	25.2 (9)	2.0 (7)	1.2 (9)	4.0 (8)	1.3 (3)	6.6 (1)	6, 42, 85
198103	VY Mic				2.4	2.0	2.2	4.4	26.0	14.0					6, 61, 69
	V577 Oph		0.939 (6)			1.6									6, 9, 88
155002	V2365 Oph	87.4 (1)	0.538 (3)	0.346	2.0 (02)		1.1 (01)	2.2 (01)	35.0 (4.0)	1.3 (03)	0.9 (1)	4.4	17.5	17.5	6, 28, 42, 85
293808	FL Ori	84.5	0.900	0.549	2.9	1.9	2.1	2.2	18.6 3.2						6, 42, 69, 84
248406	FR Ori	83.2 (1)	0.325 (2)	0.735	1.8	0.6	1.8	1.6					5.2		6, 84
252973	V392 Ori	79.8 (03)	0.247 (1)	0.951	2.0 (2)	0.5 (05)	2.0 (07)	1.3 (04)	16.9 (8)	0.5 (02)			3.6 (1)		6, 86
	MX Pav	77.0	0.150												5, 6, 61
	BG Peg	83.2 (1)	0.233 (3)	0.582	2.2	0.5	2.0	2.4					9.2		71
275604	AB Per														32, 33, 85
	IU Per	78.8 (4)	0.273 (50)	0.762	2.2	0.6	2.0	1.5	19.1 1.1				5.4	5.4	6, 36, 84
	AO Ser	87.0 (1)	0.396 (82)	0.846	2.4	1.0	1.8	1.5	17.5 0.8	1.6	5.0		5.8		6, 23
	UZ Sge	88.8 (1)	0.140 (100)	0.396	2.1 (2)	0.3 (2)	1.9 (2)	2.2 (2)	19.0 (4)	1.9 (4)	1.6 (2)	4.0 (1)	1.2 (8)	8.6 (6)	41
	AC Tau						0.0								6, 16, 42
	IZ Tel						0.0								6, 61, 82
12211	X Tri	87.9 (1)	0.599 (200)	0.724	2.1	1.3									6, 52, 85
115268	IO UMa	78.3 (1)	0.135 (3)	0.342	2.1 (1)	0.3 (02)	3.0 (04)	3.9 (05)	1.5 (04)	0.7 (07)	1.1 (1)	3.1 (2)	17.6 (1)		6, 72, 85
	VV UMa	80.9 (03)	0.337 (2)	0.722			1.7	1.4					4.9		6, 21, 47, 84
	AW Vel														6, 58
	BF Vel	86.2 (1)	0.424 (19)	0.814	2.0 (2)	0.8 (08)	1.8 (01)	1.5 (01)	15.2 (4)	1.8 (02)	1.8	4.1	4.7		6, 55
	CoRot 105906206	81.4 (1)	0.574 (8)	0.720	2.3 (04)	1.3 (03)	4.2 (02)	1.3 (01)					15.3 (1)		6, 11
172189	GSC 455-1084	73.2 (6)	0.960 (1)	0.621	1.8 (2)	1.7 (2)	4.0 (1)	2.4 (07)	52.4 (2.9)	22.2 (1)			20.3 (1)		10, 42
232486	GSC 3671-1094														6, 18, 42, 85
	GSC 3889-202														6, 13
	GSC 4293-432														15
	GSC 4588-883	78.5 (2)													6, 14
062571	GSC 4843-2140	73.0	0.662 (16)												29, 42
220687	GSC 5825-1038														6, 61
	KIC 3858884		0.999 (5)	0.213	1.9 (03)	1.9 (04)	3.5 (01)	3.1 (01)					57.2 (2)		6, 54, 85
181469	KIC 4150611														6, 66, 85
	KIC 4544587	87.9 (03)	0.810 (12)	0.689	2.0 (1)	1.6 (06)	1.8 (03)	1.6 (03)					1.6		6, 24
	KIC 4739791	72.6 (02)	0.070	0.740	1.8 (1)	0.1 (06)	1.7 (03)	0.9 (02)	10.0 (1.0)	0.6 (1)	2.3 (1)	5.2 (2)			49
	KIC 6220497	77.3 (3)	0.243 (10)	0.871	1.6 (8)	0.4 (2)	2.7 (6)	1.7 (4)	18.0 (2)	0.6 (1)	1.6 (1)	5.3 (2)			48
	KIC 6629588				1.2 (3)	1.8 (7)									51, 79
	KIC 8569819	89.9 (1)	0.588		1.7	1.0							44.6		39
	KIC 9851944	74.5 (02)	1.010 (30)	0.432	1.8 (1)	1.8 (07)	2.3 (03)	3.2 (04)					10.7 (1)	10.7 (1)	22
	KIC 10619109				1.5 (3)	2.1 (8)									51, 79
	KIC 10661783	82.4 (2)	0.091	0.744	2.1 (03)	0.2	2.6 (02)	1.1 (02)			1.4	4.3 (1)			6, 50, 67

Table A1. *– continued*

HD	Name	i (^{0})	q	f	M_p ($M_\odot$)	M_s ($M_\odot$)	R_p ($R_\odot$)	R_s ($M_\odot$)	L_p ($L_\odot$)	L_s ($L_\odot$)	$M_{bol,\,p}$ (mag)	$M_{bol,\,s}$ (mag)	a_p ($R_\odot$)	a_s ($R_\odot$)	References
	KIC 10686876				1.9 (2)	2.4 (8)									51, 79
	KIC 11401845														19
	KIC 11175495				2.0 (3)	3.1 (5)									51, 79
	TYC 7053-566-1	71.13	0.236 (4)	0.337	1.7 (1)	0.4 (03)	2.4 (07)	4.2 (11)							6, 60
	USNO-A2.0 1200-03937339	84.6 (2)	0.190 (20)	0.760	1.6 (2)	0.3 (1)	2.2 (04)	1.4 (03)	12.4 (5)	0.7 (1)	1.0 (1)	5.0 (1)			44

Notes. 1 - Alecian et al. (2005), 2 - Alfonso-Garzón et al. (2014), 3 - Bohm et al. (2008), 4 - Budding & Butland (2011), 5 - Budding et al. (2004), 6 - Casertano et al. (2017), 7 - Chapellier et al. (2004) 8 - Christiansen et al. (2007), 9 - Creevey et al. (2010), 10 - Creevey et al. (2009), 11 - da Silva et al. (2014), 12 - Dal & Sipahi (2013), 13 - Dimitrov, Kraicheva & Popov (2008), 14 - Dimitrov, Kraicheva & Popov (2009a), 15 - Dimitrov, Kraicheva & Popov (2009b), 16 - Dvorak (2009), 17 - Erdem & Öztürk (2016), 18 - Escolà-Sirisi et al. (2005), 19 - Gaulme & Guzik (2014), 20 - Griffin & Boffin (2003), 21 - Gunsriwiwat & Mkrtichian (2015) 22 - Guo et al. (2016), 23 - Hambálek (2015), 24 - Hambleton et al. (2013), 25 - Hambsch et al. (2010), 26 - Hong et al. (2015), 27 - Hosseinzadeh et al. (2014), 28 - Ibanoğlu et al. (2008) 29 - Kacar (2012), 30 - Khaliullin & Kozyreva (1989), 31 - Kim et al. (2010), 32 - Kim, Lee & Lee (2006), 33 - Kim et al. (2004), 34 - Kim et al. (2003), 35 - Kim et al. (2002), 36 - Kundra, Hric & Gális (2013), 37 - Koo et al. (2016), 38 - Korda, Zasche & Kučáková (2015), 39 - Kurtz et al. (2015), 40 - Liakos et al. (2008), 41 - Liakos & Niarchos (2012), 42 - Liakos et al. (2012), 43 - Liakos & Niarchos (2013), 44 - Liakos & Cagaš (2014), 45 - Lampens et al. (2004), 46 - Lázaro et al. (2001), 47 - Lázaro et al. (2001), 48 - Lee et al. (2016b), 49 - Lee et al. (2016a), 50 - Lehmann et al. (2013), 51 - Liakos & Niarchos (2017), 52 - Liakos, Zasche & Niarchos (2010), 53 - Liu et al. (2012), 54 - Maceroni et al. (2014), 55 - Manimanis, Vamvatira-Nakou & Niarchos (2009), 56 - Manzoori & Salar (2016), 57 - Mkrtichian & Gamarova (2000), 58 - Moriarty et al. (2013), 59 - Narusawa (2013), 60 - Norton et al. (2016), 61 - Pigulski & Michalska (2007), 62 - Popper (1988), 63 - Rodríguez et al. (2010), 64 - Russo & Milano (1983), 65 - Senyüz & Soydugan (2008), 66 - Shibahashi & Kurtz (2012), 67 - Southworth et al. (2011), 68 - Soydugan et al. (2003), 69 - Soydugan et al. (2006b), 70 - Soydugan & Soydugan (2007), 71 - Soydugan et al. (2011), 72 - Soydugan et al. (2013), 73 - Soydugan & Kaçar (2013), 74 - Soydugan et al. (2016), 75 - Tkachenko, Lehmann & Mkrtichian (2009), 76 - Tkachenko, Lehmann & Mkrtichian (2010), 77 - Turcu, Pop & Moldovan (2008), 78 - Turcu et al. (2011), 79 - Van Eylen, Winn & Albrecht (2016), 80 - van Leeuwen (2007), 81 - Yang, Wei & Li (2014), 82 - Zasche (2011), 83 - Zhang (2008), 84 - Zhang et al. (2013), 85 - Zhang, Luo & Wang (2015a), 86 - Zhang et al. (2015b), 87 - Zhang et al. (2014), 88 - Zhou (2001), 89 - Zwitter et al. (2003).

This paper has been typeset from a TEX/LATEX file prepared by the author.